Human Molecular Genetics, 2003, Vol. 12, No. 5 527–534
DOI: 10.1093/hmg/ddg043

Worldwide distribution and broader clinical spectrum of muscle–eye–brain disease

Kiyomi Taniguchi[1], Kazuhiro Kobayashi[1], Kayoko Saito[2], Hideo Yamanouchi[3], Akira Ohnuma[4], Yukiko K. Hayashi[5], Hiroshi Manya[6], Dong Kyu Jin[7], Munhyang Lee[7], Enrico Parano[8], Raffaele Falsaperla[9], Piero Pavone[9], Rudy Van Coster[10], Beril Talim[11], Alice Steinbrecher[13], Volker Straub[13], Ichizo Nishino[5], Haluk Topaloglu[12], Thomas Voit[13], Tamao Endo[6] and Tatsushi Toda[1,*]

[1]Division of Functional Genomics, Department of Post-Genomics and Diseases, Osaka University Graduate School of Medicine, 2-2-B9 Yamadaoka, Suita, Osaka 565-0871, Japan, [2]Department of Pediatrics, Tokyo Women's Medical University, School of Medicine, Tokyo, Japan, [3]Department of Pediatrics, Dokkyo University School of Medicine, Tochigi, Japan, [4]Division of Pediatric Neurology, Miyagi Prefectural Takuto Rehabilitation Centre for Children, Sendai, Japan, [5]Department of Neuromuscular Research, National Institute of Neuroscience, National Center of Neurology and Psychiatry, Tokyo, Japan, [6]Glycobiology Research Group, Tokyo Metropolitan Institute of Gerontology, Tokyo, Japan, [7]Department of Pediatrics, Sungkyunkwan University, Samsung Medical Center, Seoul, South Korea, [8]Institute of Neurological Science, The National Research Council of Italy, Catania, Italy, [9]Pediatric Clinic, University of Catania, Catania, Italy, [10]Division of Neurometabolic Disorders, Ghent University Hospital, Ghent, Belgium, [11]Department of Pediatric Pathology and [12]Department of Pediatric Neurology, Hacettepe Children's Hospital, Ankara, Turkey and [13]Department of Pediatrics and Pediatric Neurology, University of Essen, Essen, Germany

Received November 1, 2002; Revised and Accepted December 19, 2002 DDBJ/EMBL/GenBank accession no. AB057356

Muscle–eye–brain disease (MEB), an autosomal recessive disorder prevalent in Finland, is characterized by congenital muscular dystrophy, brain malformation and ocular abnormalities. Since the MEB phenotype overlaps substantially with those of Fukuyama-type congenital muscular dystrophy (FCMD) and Walker–Warburg syndrome (WWS), these three diseases are thought to result from a similar pathomechanism. Recently, we showed that MEB is caused by mutations in the protein *O*-linked mannose β1,2-*N*-acetylglucosaminyltransferase 1 (*POMGnT1*) gene. We describe here the identification of seven novel disease-causing mutations in six of not only non-Finnish Caucasian but also Japanese and Korean patients with suspected MEB, severe FCMD or WWS. Including six previously reported mutations, the 13 disease-causing mutations we have found thus far are dispersed throughout the entire *POMGnT1* gene. We also observed a slight correlation between the location of the mutation and clinical severity in the brain: patients with mutations near the 5′ terminus of the *POMGnT1* coding region show relatively severe brain symptoms such as hydrocephalus, while patients with mutations near the 3′ terminus have milder phenotypes. Our results indicate that MEB may exist in population groups outside of Finland, with a worldwide distribution beyond our expectations, and that the clinical spectrum of MEB is broader than recognized previously. These findings emphasize the importance of considering MEB and searching for *POMGnT1* mutations in WWS or other congenital muscular dystrophy patients worldwide.

*To whom correspondence should be addressed at: Division of Functional Genomics, Department of Post-Genomics and Diseases, Osaka University Graduate School of Medicine, 2-2-B9 Yamadaoka, Suita, Osaka 565-0871, Japan. Tel: +81 668793380; Fax: +81 668793389; Email: toda@clgene.med.osaka-u.ac.jp

INTRODUCTION

Muscle–eye–brain disease (MEB: MIM 253280) is an autosomal recessive disorder characterized by congenital muscular dystrophy (CMD), ocular abnormalities and brain malformation (type II lissencephaly) (1). Patients with MEB show congenital muscular dystrophy, severe congenital myopia, congenital glaucoma, pallor of the optic discs, retinal hypoplasia, mental retardation, hydrocephalus, abnormal electroencephalograms and myoclonic jerks. From birth, infants with MEB are floppy with generalized muscle weakness, including facial and neck muscles. Muscle biopsies show dystrophic changes, and brain MRIs reveal pachygyria-type cortical neuronal migration disorder, flat brainstem and cerebellar hypoplasia. Walker–Warburg syndrome (WWS: MIM 236670) is another extreme of CMD, which shows the most severe brain malformation, characterized by type II lissencephaly and eye involvement. WWS is usually lethal within the first year of life (2). Fukuyama-type congenital muscular dystrophy (FCMD: MIM 253800) is a recessively inherited CMD with type II lissencephaly that occurs exclusively in Japan (3). In some cases, the clinical resemblance makes it difficult to differentiate between MEB, FCMD and WWS. These three diseases are thought to be caused by a similar pathomechanism.

Molecular genetic studies have been helpful in defining subgroups of CMD. The genes responsible for both MEB and FCMD have been identified and characterized. Through linkage analysis, the gene responsible for MEB was localized to chromosome 1p32–34 (4), and we recently showed that MEB is caused by loss of function mutations in the gene encoding protein *O*-linked mannose β1,2-*N*-acetylglucosaminyltransferase 1 (POMGnT1) (5). *O*-mannosylation is a rare type of glycosylation in mammals, occurring in a limited number of brain, nerve and skeletal muscle glycoproteins (6). Sialyl *O*-mannosyl glycan is known to be a laminin-binding ligand of α-dystroglycan (7), and POMGnT1 catalyzes the transfer of *N*-acetylglucosamine to *O*-mannose of glycoproteins.

FCMD is caused by mutations in the *fukutin* gene on chromosome 9q31, which we positionally cloned previously (8–11). The function of fukutin is not yet clear; however, sequence analysis predicts it to be an enzyme that modifies cell-surface glycoproteins or glycolipids (12). Immunoreactivity to the glycans of α-dystroglycan has been undetectable in skeletal muscle from both MEB and FCMD patients (13–15), and the core α-dystroglycan protein shows an electrophoretic mobility shift (15). These findings have suggested a common pathomechanism for MEB and FCMD, in which defects in *O*-mannosylation compromise laminin binding. Identification of the genes responsible for MEB and FCMD now enables the definition of these complicated diseases at the molecular level, since their symptoms are often similar and complicated. In particular genetic analysis of FCMD is being performed frequently and has been highly informative (16).

WWS has been observed in many population groups with a worldwide distribution. In contrast, both MEB and FCMD show striking founder effects. MEB was first described in Finland, where it is most prevalent, owing to a strong founder effect followed by genetic drift (17). Consequently, most MEB patients have come from a small, geographically isolated population in Finland, with few Caucasian exceptions. Most FCMD mutations can be traced to a single ancestral founder, who carried a 3 kb retrotransposal insertion in the 3′ non-coding region of the *fukutin* gene (11,18). Thus far, FCMD patients have been identified exclusively in Japan.

We describe here the identification of different MEB-causing mutations in Japanese and Korean patients as well as Caucasian patients initially diagnosed as FCMD, MEB, or WWS. Our results show that MEB is present in diverse population groups with a worldwide distribution and has a broader clinical spectrum than previously expected. Furthermore, we have shown a slight genotype–phenotype correlation in the brain among the patients.

RESULTS

Patients and mutation analysis

In a previous study, we showed that mutations in the *POMGnT1* gene are the primary genetic defect in MEB. Mutation analysis and characterization of the gene product has demonstrated that MEB is inherited in a loss-of-function manner (5). In this study, we extended our analysis to screen the entire coding region and exon/intron flanking sequences of the *POMGnT1* gene for mutations in 30 patients who were clinically diagnosed for WWS, severe FCMD, or MEB. To determine whether MEB patients exist in Asia, we included Japanese and Korean patients in this study.

Our analysis identified seven novel mutations and one recurrent mutation in six patients (Fig. 1, Table 1). None of these individuals harbored mutations in the *fukutin* gene. Combined with our previous results, we have now identified a total of 13 different mutations in the *POMGnT1* gene.

Patient EV carried a homozygous C281T transition in exon 3, which results in an Arg63Stop nonsense mutation (Fig. 1A). EV is a 12-year-old Italian female who was hospitalized at one year of age for a ventriculo-peritoneal shunt operation for hydrocephalus. She is unable to speak or walk (Table 2).

Patient HS is a 12-year-old Japanese male. He is a compound heterozygote who carried a 1 bp deletion at base 541 in exon 6 (frameshift and premature termination at codon 167) and a G761A transition in exon 8 (Glu223Lys) (Fig. 1B). Severe hydrocephalus was observed prenatally by an ultrasonograph, and an MR image at 6 years of age showed extreme ventricular dilatation and agenesis of the septum pellucidum (Fig. 3A). Of all the patients examined, HS showed one of the more severe phenotypes (Table 2).

SI, a 7-year-old female Japanese patient, was identified as a compound heterozygote with a G900A transition in exon 9 (Cys269Tyr) and a 1 bp insertion at base 1077 in exon 11 (frameshift and premature termination at codon 338; Fig. 1C). Dilated ventricles were observed prenatally by an ultrasonograph, and, at one year of age, hydrocephalus required a ventriculo-peritoneal shunt. SI also shows a more severe phenotype (Table 2).

Patient DC, an 8-year-old Belgian female, is compound heterozygous for a G761A transition in exon 8 (Glu223Lys) and a G-to-A substitution in intron 17, which alters the conserved GT splicing donor sequence to AT (Fig. 1D). In our

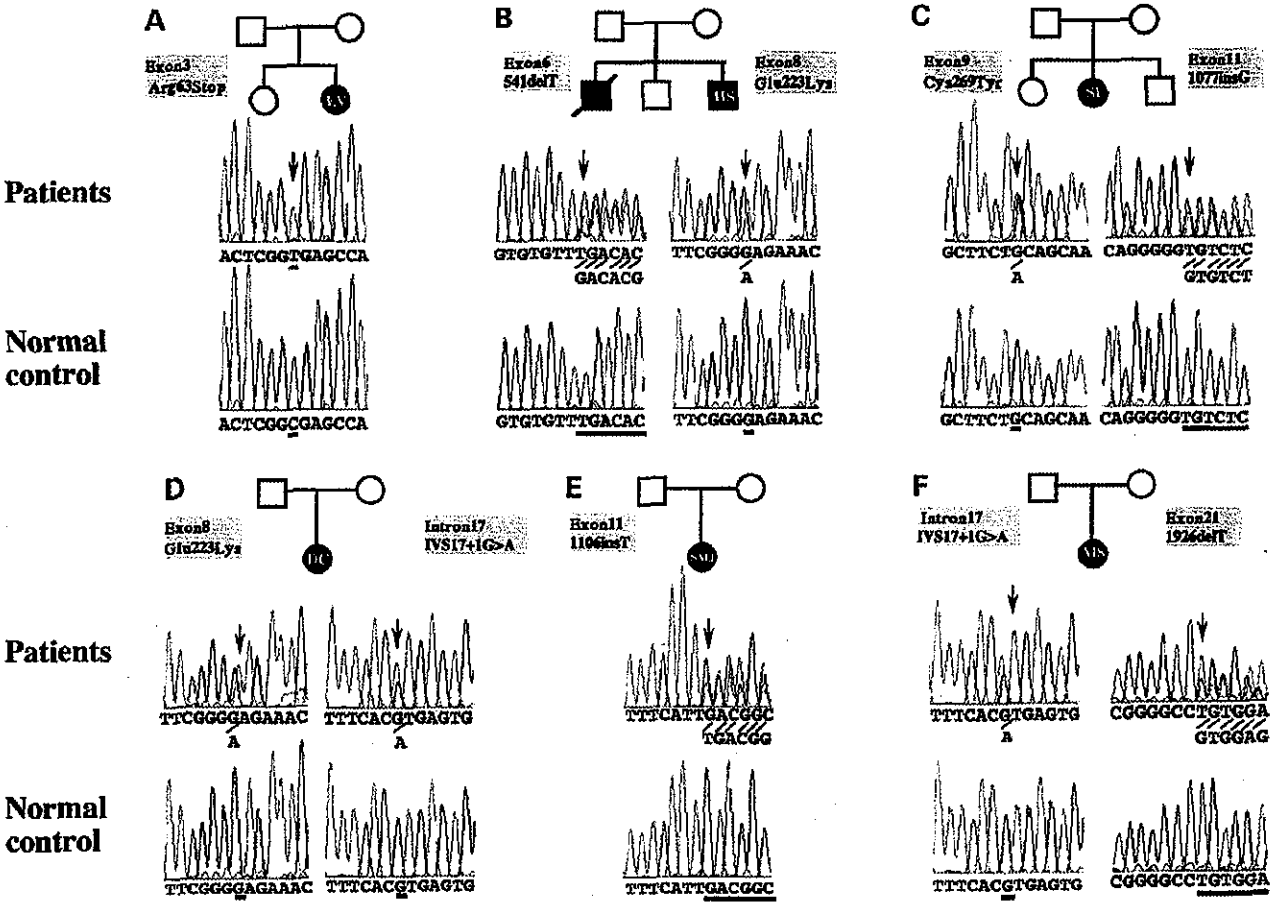

Figure 1. Novel point mutations in six patients with MEB. (A) Patient EV carried a homozygous C281T transition in exon 3, which results in an Arg63Stop nonsense mutation. (B) Patient HS is a compound heterozygote who carries a 1 bp deletion at base 541 in exon 6 (frameshift) and a G761A transition in exon 8 (Glu223Lys). (C) Patient SI is compound heterozygous for a G900A transition in exon 9 (Cys269Tyr) and a 1 bp insertion at base 1077 in exon 11 (frameshift). (D) Patient DC is compound heterozygous for a G761A transition in exon 8 (Glu223Lys) and a G-to-A substitution in intron 17, which causes abnormal splicing. (E) Patient SMJ was shown to be a putative compound heterozygote who carries a 1 bp insertion at base 1106 in exon 11 (frameshift). Thus far, no coding region mutation has been detected in the other allele. (F) Patient MS is compound heterozygous for a G-to-A substitution in intron 17 (abnormal splicing) and a 1 bp deletion at base 1926 in exon 21 (frameshift).

Table 1. Summary of novel mutations of the *POMGnT1* gene in MEB patients

Patients	Mutation	Location	Effect	Status
EV	281C>T	Exon3	Arg63Stop Nonsense	Homozygote
HS	541 del T	Exon6	Phe149 frameshift 167Stop	Compound heterozygote
	761G>A	Exon8	Glu223Lys Missense	
SI	900G>A	Exon9	Cys269Tyr Missense	Compound heterozygote
	1077 ins G	Exon11	Val328 frameshift 338Stop	
DC	761G>A	Exon8	Glu223Lys Missense	Compound heterozygote
	IVS17+1G>A[a]	Intron17	Glu514read-through 526Stop/Leu472-His513del	
SMJ	1106 ins T	Exon11	Asp338 frameshift 338Stop	Compound heterozygote
	?	Noncoding region?	?	
MS	IVS17+1G>A[a]	Intron17	Glu514read-through 526Stop/Leu472-His513del	Compound heterozygote
	1926 del T	Exon21	Leu611 frameshift 633Stop	

[a]Mutation was reported in the previous study (5).

Table 2. Clinical features of MEB patients

Patient	EV	HS	SI	DC	SMJ	KO[a]	YA[a]	SA[a]	MK[a]	CC[a]	MS	TLG[a]
Origin	Italy	Japan	Japan	Belgium	Korea	Turkey	Turkey	Turkey	Turkey	Turkey	USA/Japan	France
Age (years)	12	12	7	8	6	12	6	7	5	10	25	3
Clinical diagnosis	Atypical WWS	WWS or MEB	MEB or severe FCMD	FCMD or MEB	FCMD	MEB	MEB	MEB	MEB	MEB	A milder WWS	MEB
Mutation (location)	Arg63Stop (exon 3)	541delT (exon 6)	Cys269Tyr (exon 9)	Glu223Lys (exon 8)	1106insT (exon 11)	IVS17+ 1G>T (intron 17)	IVS17+ 1G>T (intron 17)	IVS17+ 1G>A (intron 17)	Ser535-Ser550 del (exon 19)	1813delC (exon 20)	IVS17+ 1G> (intron 17)	Pro493Arg (exon 17)
		Glu223Lys (exon 8)	1077insG (exon 11)	IVS17+ 1G>A (intron 17)	ni (noncoding?)						1926delT (exon 21)	1970delG (exon 21)
Brain												
Mental retardation	+++	+++	+++	+++	ni	+++	++	++	+++	+++	++	+++
Speech	No words	No words	No words	Single words	No words	No words	No words	ni	ni	No words	A single word	No words
IQ/DQ	IQ < 30	DQ < 10	DQ < 20	IQ~30	ni	ni	ni	ni	ni	ni	DQ~43	ni
Hydrocephalus	√	√	√	√	—	√	ni	—	—	—	—	ni
Brainstem hypoplasia	+++	+++	++	+++	ni	+++	++	++	+++	+	+	+++
Septum pellucidum agenesis	—	√	√	—	—	√	ni	—	—	—	—	ni
Corpus callosum hypoplasia	—	√	√	—	√	√	ni	√	√	√	—	ni
White matter lucency	—	—	++	++	—	++	++	+	++	++	++	+
Type II lissencephaly	++	++	++	++	—	++	ni	+++	+++	+	++	++
Cerebellar vermis hypoplasia	√	√	—	—	√	√	√	√	√	√	√	ni
Eyes												
Myopia	√	√	√	√	ni	√	ni	ni	—	√	√	√
Retinal dysplasia	√	√	√	—	ni	—	ni	ni	√	—	√	—
Anterior chamber malformation	—	—	—	—	ni	√	√	ni	—	√	—	—
Microphthalmia	—	—	√	—	ni	—	√	ni	—	—	—	—
High VEP	—	√	√	—	ni	ni	ni	—	ni	ni	√	—
Muscle												
Maximum motor function (age)	Sit with support (10 years)	Head control (8 years)	No head control (7 years)	Sit with support (2 years)	ni	No Head control (12 years)	Head control (4 years)	head control (3 years)	No head control (8 years)	Sit with support (5 years)	Sit with support (3 years)	No head control (3 years)
CK(U/l) (age)	700 (10 years)	2365 (6 years)	852 (6 years)	1844 (ni)	ni	42271 (2 years)	434 (10 months)	844 (4 years)	628 (4 years)	1212 (3 years)	1339 (12 years)	4778 (1 year)

[a]Patients whose mutations were reported in the previous study (5). +++, severe; ++, moderate; +, mild; √, observed; —, not observed; ni, no information was obtained in these patients.

previous study, we found that the intron 17 mutation caused both read-through of intronic sequences, resulting in introduction of a premature termination codon, and skipping of the upstream exon 17, resulting in the deletion of 42 amino acids (5). In DC, severe myopia was found upon opthalmological examination in the first months of life, although retinal dysplasia was not observed. Although she was able to sit with support and her speech was limited to three single words at 2 years of age, by 7 years of age she was severely hypotonic and mentally retarded. DC shows a relatively mild phenotype compared with the other patients examined (Table 2).

A 6-year-old female Korean patient, SMJ is a putative compound heterozygote who carried a 1 bp insertion at base 1106 in exon 11, causing a frameshift and premature termination at codon 338 (Fig. 1E). We were unable to detect a mutation in the other *POMGnT1* allele. It is possible that the second mutation may lie outside the coding sequence, perhaps in the promoter or a regulatory region of an intron.

Patient MS is the 25-year-old female child of a Japanese mother and an American father of Scandinavian origin (19). The *POMGnT1* allele inherited from her father harbors a G-to-A substitution in intron 17, which alters the GT splicing sequence. From her mother, MS inherited a 1 bp deletion at base 1926 in exon 21, which results in a frameshift and premature termination at codon 633 (Fig. 1F). MS was previously diagnosed with a milder form of WWS because her symptoms included relatively severe eye abnormalities and specific features such as severe hypoplasia of the cerebellar vermis and cataracts, which are common in WWS. However her mental retardation is relatively mild for MEB and she can indicate 'yes' or 'no' with gestures (Table 2).

In each case, mutations cosegregated within the pedigree (families HS, SI, SMJ, and MS). We screened at least 92 normal individuals for two missense changes (Cys269Tyr and Glu223Lys), excluding the possibility of polymorphism.

In addition, patient MK is one of the subjects examined in our previous report (5). MK is a 5-year-old Turkish male who does not show MEB-specific eye symptoms such as myopia. MK carried a homozygous G1743A transition in the final base of exon 19, which was previously reported as a missense mutation (Ser550Asn) (5). However, subsequent RT–PCR analysis of skeletal muscle from this patient has shown that this mutation causes skipping of exon 19, resulting in the deletion of 15 amino acids (data not shown).

Genotype–phenotype correlation

We found that patients with MEB showed a broad range of severity of symptoms. In addition, we found that these patients possessed mutations that were scattered throughout the *POMGnT1* gene. To assess whether there is a genotype–phenotype correlation, we investigated the clinical features of the patients with regard to brain, eye and muscle, relative to the distribution of mutations throughout the *POMGnT1* gene (Table 2, Fig. 2). This analysis revealed a wider clinical spectrum of MEB than recognized previously. Taking into account each patient's clinical features, correlations between the location of the mutation and clinical severity seemed difficult to assess. However, a slight correlation of clinical severity in the brain was observed. Patients with mutations near the 5′ terminus of the *POMGnT1* coding region showed relatively severe brain symptoms, while patients with mutations near the 3′ terminus had milder phenotypes. (Table 2). Hydrocephalus showed a particular correlation with mutations near the 5′ terminus (Table 2, Fig. 3). For example, patient HS, who carried a 1 bp deletion in exon 6 and a missense mutation in exon 8, near the 5′ terminus, was diagnosed as WWS or MEB and showed relatively severe phenotypes such as hydrocephalus (Table 2, Fig. 3A). On the other hand, patient CC carried a homozygous 1 bp deletion in exon 20, near the 3′ terminus of the *POMGnT1* coding region. CC had a relatively mild phenotype without hydrocephalus (Table 2, Fig. 3B). These analyses suggest that the location of a mutation influences the severity of the MEB phenotype.

In addition, we examined the skeletal muscle tissue from both patient SI who carried mutations near the 5′ terminus (Fig. 3C–E) and patient TLG who carried mutations near the 3′ terminus (Fig. 3F–H) and found normal immunoreactivity for β-dystroglycan and laminin α2 chain but greatly reduced staining for α-dystroglycan. No obvious differences could be observed in the skeletal muscle of the two patients.

DISCUSSION

The six *POMGnT1* mutations identified in the previous study were all simple point mutations (5), while most FCMD patients carry a quite rare insertion mutation in the *fukutin* gene and are found exclusively in Japan. These findings led us to hypothesize that MEB mutations might have a broader distribution outside Finland. A recent linkage study reported the occurrence of MEB in some Caucasians and classified MEB and WWS as distinct disorders (20). To test our hypothesis, we examined 30 patients from various countries, including Japan and Korea, who were diagnosed as WWS, severe FCMD or MEB. In addition to the six previously described mutations, we identified seven new mutations in this study. Therefore, MEB patients may exist with a broader distribution and more varied phenotypes than previously expected.

The 13 known mutations in the *POMGnT1* gene are dispersed throughout the entire coding region (Fig. 2), with no accumulation in any particular domain. The clinical features of MEB vary among patients, and evaluation of clinical severity in each individual patient is difficult. However, we observed a slight correlation between genotype and brain phenotype: patients with mutations in the vicinity of the 5′ terminus of the *POMGnT1* gene show relatively severe WWS-like symptoms. All of the patients with *POMGnT1* mutations are still alive; hence, lifespan may be one of the differences between MEB and typical WWS, in which almost patients die before one year of age.

The amino acid sequence of POMGnT1 is homologous to α-3-D-mannoside β-1,2-*N*-acetylglucosaminyltransferase I (GnT-I), which is a Golgi-resident enzyme involved in the *N*-linked oligosaccharide biosynthetic pathway. While the crystal structure of GnT-I has been determined (21), the structure of POMGnT1 itself has not been analyzed in detail. Computer analysis predicts that the 660-amino-acid POMGnT1 protein is divided into four domains: a cytoplasmic tail (Met1-Arg37), a transmembrane domain (Phe38-Ile58), a stem domain (Leu59–Leu300), the catalytic domain consisting of the UDP-GlcNAc

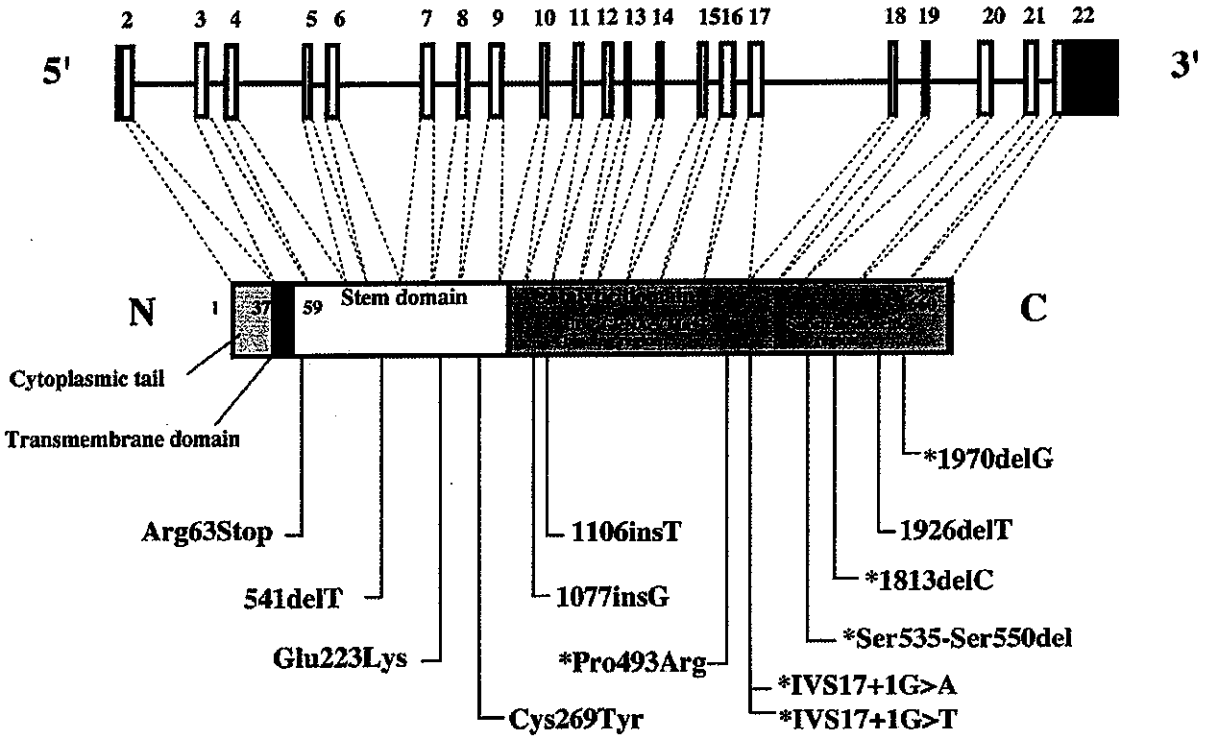

Figure 2. Schematic representation of the *POMGnT1* gene and the corresponding protein, showing the location of mutations found in MEB. Exons are represented by boxes, and introns are represented by lines. POMGnT1 protein is divided into four domains. Mutations detected in this study and in the previous study are shown below the protein. The asterisk represents mutations reported in the previous study (5).

and Mn^{2+} binding regions (around Asn301–Leu530), and the substrate-specific region (around Arg531-Thr660) (5). Nonsense or frameshift mutations near the 5′ terminus shorten the POMGnT1 protein significantly, probably resulting in loss of function. Missense mutations in the stem domain may diminish retention of POMGnT1 in the Golgi apparatus (22). Mutations in the 3′ region of the gene may retain some ability to transfer sugars, since the catalytic domain of the protein is preserved to some extent. Measurement of the enzymatic activity of mutant POMGnT1 proteins will be necessary to explain possible mechanisms for the genotype–phenotype correlation seen in this study.

MEB, FCMD and WWS are clinically similar, and the nosological classification of these disorders has been controversial. In MEB and FCMD patients, the lack of full *O*-mannosylation of α-dystroglycan significantly disrupts the interactions of α-dystroglycan with extracellular matrix ligands (15). This result suggests that post-translational disruption of dystroglycan–ligand interactions may be a common mechanism for muscular dystrophy with brain abnormalities. The structure of laminin-binding *O*-mannosyl glycan in dystroglycan is Siaα2-3Galβ1-4GlcNAcβ1-2Man-Ser/Thr (7), where POMGnT1 catalyzes the GlcNAcβ1-2Man linkage (5). Since the clinical presentations of MEB and WWS significantly overlap, and the most severe brain malformation and shortest life span are striking features of WWS, we postulated that the gene product responsible for WWS may be a glycosyltransferase that catalyzes the Man-Ser/Thr linkage in *O*-mannosyl glycans. Quite recently 20% of WWS patients have been found to have mutations in *POMT1*, a putative human counterpart of a yeast *O*-mannosyltransferase (23). In FCMD, compound heterozygotes for the FCMD founder mutation in the *fukutin* gene show severe phenotypes like WWS, and no patients have been identified with non-founder (point) mutations on both alleles, suggesting that such patients are embryonic lethal (16,24). Unlike FCMD, MEB patients with point mutations on both alleles can survive. We suppose that fukutin may perform a more essential role in early development than POMGnT1.

Further molecular genetic study will open new avenues for understanding the pathophysiological mechanisms underlying these complex disorders. It may be necessary and possible to re-classify muscular dystrophies based on genetic rather than clinical criteria. This study emphasizes the importance of considering MEB and searching for *POMGnT1* mutations in WWS or other CMD patients worldwide.

MATERIALS AND METHODS

Patients

We analyzed genomic DNA from 30 patients with CMD, brain malformation and ocular abnormalities. Information about the

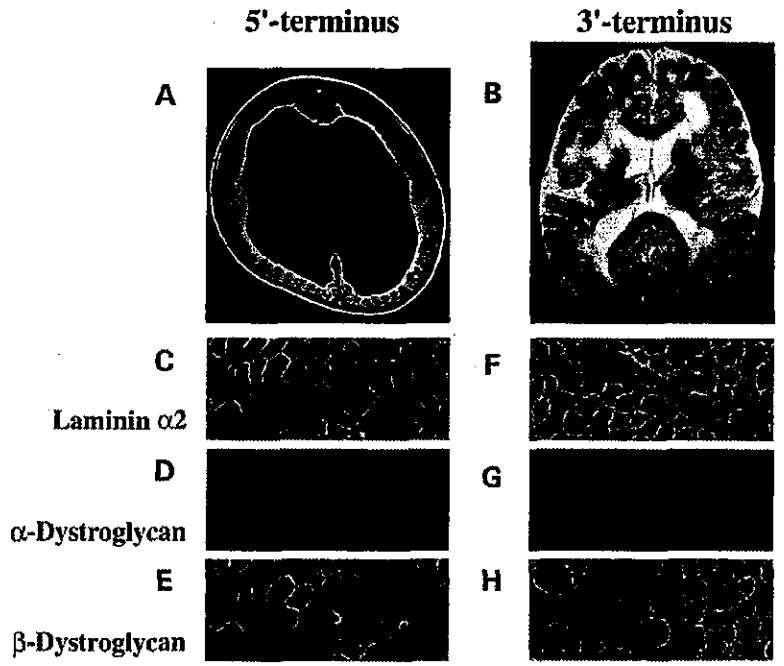

Figure 3. Comparison of cranial MR images and immunohistochemical analysis in MEB patients. **(A)** An axial T_1-weighted image of patient HS (at 6 years of age) shows extreme ventricular dilatation with a slightly smooth cortical surface. **(B)** An axial T_2-weighted image of patient CC (at 13 months of age) shows pachygyria, slightly enlarged ventricles, and white matter abnormality. The mutation in patient CC has been reported previously (5). Consecutive frozen sections of skeletal muscle from patient SI (C–E) and patient TLG (F–H) immunostained with anti-laminin α2 chain (C, F), α-dystroglycan (D, G), and β-dystroglycan antibodies (E, H).

six patients whose mutations were identified in this study (EV, HS, SI, DC, SMJ and MS) is briefly described in the Results section. All parents of these patients are not consanguineous. The six patients KO, YA, SA, MK, CC and TLG were described in the previous study (5). All phenotypes are summarized in Table 2.

Mutation analysis

Primers used for mutation analysis have been described previously (5). PCR products from patient genomic DNA were excised from gels, and direct sequencing was performed using Bigdye terminators (Applied Biosystems). Fragments were electrophoresed on an ABI Prism 3100 sequencer (Applied Biosystems).

Immunohistochemistry

Immunodetection was performed using a mouse monoclonal anti-α-dystroglycan antibody for patient SI (clone VIA4-1, Upstate Biotechnology), affinity-purified sheep antiserum directed against a 20-amino-acid C-terminal sequence of chick α-dystroglycan (25) for patient TLG, a monoclonal anti-β-dystroglycan (clone 8D5, Novocastra), a polyclonal anti-β-dystroglycan (26) and a monoclonal anti-laminin α2 chain antibody (clone 5H2, GibcoBRL, Chemicon). Skeletal muscle staining was performed as described previously (13).

ACKNOWLEDGEMENTS

We thank Dr Jennifer Logan and Ms Helena A. Popiel for editing the manuscript. This study was supported by Health Science Research Grant, 'Research on Brain Science' (H12-Brain-017) and by a Research Grant for Nervous and Mental Disorders (11B-1), both from the Ministry of Health, Labor and Welfare of Japan, and a Grant-in-Aid for Scientific Research (C) (13672376) from the Japan Society for the Promotion of Science.

REFERENCES

1. Santavuori, P., Somer, H., Sainio, K., Rapola, J., Kruus, S., Nikitin, T., Ketonen, L. and Leisti, J. (1989) Muscle-eye-brain disease (MEB). *Brain Devl.*, **11**, 147–153.
2. Dobyns, W.B., Pagon, R.A., Armstrong, D., Curry, C.J., Greenberg, F., Grix, A., Holmes, L.B., Laxova, R., Michels, V.V., Robinow, M. *et al.* (1989) Diagnostic criteria for Walker–Warburg syndrome. *Am. J. Med. Genet.*, **32**, 195–210.
3. Fukuyama, Y., Osawa, M. and Suzuki, H. (1981) Congenital progressive muscular dystrophy of the Fukuyama type—clinical, genetic and pathological considerations. *Brain Devl.*, **3**, 1–29.
4. Cormand, B., Avela, K., Pihko, H., Santavuori, P., Talim, B., Topaloglu, H., de la Chapelle, A. and Lehesjoki, A.E. (1999) Assignment of the muscle–eye–brain disease gene to 1p32-p34 by linkage analysis and homozygosity mapping. *Am. J. Hum. Genet.*, **64**, 126–135.
5. Yoshida, A., Kobayashi, K., Manya, H., Taniguchi, K., Kano, H., Mizuno, M., Inazu, T., Mitsuhashi, H., Takahashi, S., Takeuchi, M. *et al.* (2001) Muscular dystrophy and neuronal migration disorder caused by mutations in a glycosyltransferase, POMGnT1. *Devl. Cell*, **1**, 717–724.

6. Endo, T. (1999) *O*-mannosyl glycans in mammals. *Biochim. Biophys. Acta*, **1473**, 237–246.
7. Chiba, A., Matsumura, K., Yamada, H., Inazu, T., Shimizu, T., Kusunoki, S., Kanazawa, I., Kobata, A. and Endo, T. (1997) Structures of sialylated *O*-linked oligosaccharides of bovine peripheral nerve α-dystroglycan. The role of a novel *O*-mannosyl-type oligosaccharide in the binding of α-dystroglycan with laminin. *J. Biol. Chem.*, **272**, 2156–2162.
8. Toda, T., Segawa, M., Nomura, Y., Nonaka, I., Masuda, K., Ishihara, T., Sakai, M., Tomita, I., Origuchi, Y., Suzuki, M. *et al.* (1993) Localization of a gene for Fukuyama type muscular dystrophy to chromosome 9q31-33. *Nat. Genet.*, **5**, 283–286.
9. Toda, T., Ikegawa, S., Okui, K., Kondo, E., Saito, K., Fukuyama, Y., Yoshioka, M., Kumagai, T., Suzumori, K., Kanazawa, I. *et al.* (1994) Refined mapping of a gene responsible for Fukuyama-type congenital muscular dystrophy: evidence for strong linkage disequilibrium. *Am. J. Hum. Genet.*, **55**, 946–950.
10. Toda, T., Miyake, M., Kobayashi, K., Mizuno, K., Saito, K., Osawa, M., Nakamura, Y., Kanazawa, I., Nakagome, Y., Tokunaga, K. *et al.* (1996) Linkage-disequilibrium mapping narrows the Fukuyama-type congenital muscular dystrophy (FCMD) candidate region to <100 kb. *Am. J. Hum. Genet.*, **59**, 1313–1320.
11. Kobayashi, K., Nakahori, Y., Miyake, M., Matsumura, K., Kondo-Iida, E., Nomura, Y., Segawa, M., Yoshioka, M., Saito, K., Osawa, M. *et al.* (1998) An ancient retrotransposal insertion causes Fukuyama-type congenital muscular dystrophy. *Nature*, **394**, 388–392.
12. Aravind, L. and Koonin, E.V. (1999) The fukutin protein family—predicted enzymes modifying cell-surface molecules. *Curr. Biol.*, **9**, R836–R837.
13. Kano, H., Kobayashi, K., Herrmann, R., Tachikawa, M., Manya, H., Nishino, I., Nonaka, I., Straub, V., Talim, B., Voit, T. *et al.* (2002) Deficiency of α-dystroglycan in muscle–eye–brain disease. *Biochem. Biophys. Res. Commun.*, **291**, 1283–1286.
14. Hayashi, Y.K., Ogawa, M., Tagawa, K., Noguchi, S., Ishihara, T., Nonaka, I. and Arahata, K. (2001) Selective deficiency of α-dystroglycan in Fukuyama-type congenital muscular dystrophy. *Neurology*, **57**, 115–121.
15. Michele, D.E., Barresi, R., Kanagawa, M., Saito, F., Cohn, R.D., Satz, J.S., Dollar, J., Nishino, I., Kelley, R.I., Somer, H. *et al.* (2002) Post-translational disruption of dystroglycan–ligand interactions in congenital muscular dystrophies. *Nature*, **418**, 417–422.
16. Kondo-Iida, E., Kobayashi, K., Watanabe, M., Sasaki, J., Kumagai, T., Koide, H., Saito, K., Osawa, M., Nakamura, Y. and Toda, T. (1999) Novel mutations and genotype–phenotype relationships in 107 families with Fukuyama-type congenital muscular dystrophy (FCMD). *Hum. Mol. Genet.*, **8**, 2303–2309.
17. de la Chapelle, A. and Wright, F.A. (1998) Linkage disequilibrium mapping in isolated populations: the example of Finland revisited. *Proc. Natl Acad. Sci. USA*, **95**, 12416–12423.
18. Kobayashi, K., Nakahori, Y., Mizuno, K., Miyake, M., Kumagai, T., Honma, A., Nonaka, I., Nakamura, Y., Tokunaga, K. and Toda, T. (1998) Founder-haplotype analysis in Fukuyama-type congenital muscular dystrophy (FCMD). *Hum. Genet.*, **103**, 323–327.
19. Saito, K., Suzuki, H. Shishikura, K., Ozawa, M. and Fukuyama, Y. (1997) A milder form of Walker–Warburg syndrome. In Fukuyama, Y., Ozawa, M.a and Saito, K. (eds), *Congenital Muscular Dystrophies*. Elsevier, The Netherlands, pp. 345–354.
20. Cormand, B., Pihko, H., Bayés, M., Valanne, L., Santavuori, P., Talim, B., Gershoni–Baruch, R., Ahmad, A., van Bokhoven, H., Brunner, H.G. *et al.* (2001) Clinical and genetic distinction between Walker–Warburg syndrome and muscle–eye–brain disease. *Neurology*, **56**, 1059–1069.
21. Ünligil, U.M., Zhou, S., Yuwaraj, S., Sarkar, M., Schachter, H. and Rini, J.M. (2000) X-ray crystal structure of rabbit *N*-acetylglucosaminyltransferase I: catalytic mechanism and a new protein superfamily. *EMBO J.*, **19**, 5269–5280.
22. Gleeson, P.A. (1998) Targeting of proteins to the Golgi apparatus. *Histochem. Cell Biol.*, **109**, 517–532.
23. Beltrán-Valero de Bernabé, D., Currier, S., Steinbrecher, A., Celli, J., van Beusekom, E., van der Zwaag, B., Kayserili, H., Merlini, L., Chitayat, D., Dobyns, W.B. *et al.* (2002) Mutations in the *O*-mannosyltransferase gene *POMT1* give rise to the severe neuronal migrarion disorder Walker–Warburg Syndrome. *Am. J. Hum. Genet.*, **71**, 1033–1043.
24. Toda, T., Kobayashi, K., Kondo-Iida, E., Sasaki, J. and Nakamura, Y. (2000) The Fukuyama congenital muscular dystrophy story. *Neuromuscul. Disord.*, **10**, 153–159.
25. Herrmann, R., Straub, V., Blank, M., Kutzick, C., Franke, N., Jacob, E.N., Lenard, H.G., Kroger, S. and Voit, T. (2000) Dissociation of the dystroglycan complex in caveolin-3-deficient limb girdle muscular dystrophy. *Hum. Mol. Genet.*, **9**, 2335–2340.
26. Yoshida, M., Mizuno, Y., Nonaka, I. and Ozawa, E. (1993) A dystrophin-associated glycoprotein, A3a (one of 43DAG doublets), is retained in Duchenne muscular dystrophy muscle. *J. Biochem.*, **114**, 634–639.

Journal of Neurochemistry, 2003, 87, 1296–1308 doi:10.1046/j.1471-4159.2003.02132.x

Characterization of Cln3p, the gene product responsible for juvenile neuronal ceroid lipofuscinosis, as a lysosomal integral membrane glycoprotein

Junji Ezaki,* Mitsue Takeda-Ezaki,* Masato Koike,‡ Yoshiyuki Ohsawa,‡ Hikari Taka,† Reiko Mineki,† Kimie Murayama,† Yasuo Uchiyama,‡ Takashi Ueno* and Eiki Kominami*

**Department of Biochemistry and †Division of Biochemical Analysis, Central Laboratory of Medical Science, Juntendo University School of Medicine, Tokyo, Japan*

‡Department of Cell Biology and Neuroscience, Osaka University Graduate School of Medicine, Osaka, Japan

Abstract

Juvenile neuronal ceroid lipofuscinosis (JNCL) is an autosomal recessively inherited lysosomal storage disease involving a mutation in the *CLN3* gene. The sequence of *CLN3* was determined in 1995; however, the localization of the *CLN3* gene product (Cln3p) was not confirmed. In this study, we investigated endogenous Cln3p using two peptide antibodies raised against two distinct epitopes of murine Cln3p. Identification of the liver 60 kDa protein as Cln3p was ascertained by amino acid sequence analysis using tandem mass spectrometry. Liver Cln3p was predominantly localized in the lysosomal membranes, not in endoplasmic reticulum (ER) or Golgi apparatus. As the tissue concentration of brain Cln3p was much lower than that of liver Cln3p, it could be detected only after purification from brain extract using anti-Cln3p IgG Sepharose. The apparent molecular masses of liver Cln3p and brain Cln3p were determined to be about 60 kDa and 55 kDa, respectively. Both brain and liver Cln3p were deglycosylated by PNGase F treatment to form polypeptides with almost the same molecular mass (45 kDa). However, they were not affected by Endo h treatment. In addition, it was also elucidated that the amino terminal region of Cln3p faces the cytosol.

Keywords: CLN3, LC-MS, lectin, lysosomes, MS/MS, neuronal ceroid lipofuscinosis.

J. Neurochem. (2003) **87**, 1296–1308.

Neuronal ceroid lipofuscinoses (NCLs) are the most common inherited progressive neurodegenerative disorders in infants, children, and young adults, and lead to blindness, seizures, dementia, and premature death. They are characterized pathologically by the massive lysosomal storage of autofluorescent lipopigments in neurons and a wide variety of extraneuronal cells (Rider *et al.* 1992; Kida *et al.* 2001). They are genetically heterogeneous and classified into eight subtypes (Mole 1999): infantile NCL (INCL; defective gene is CLN1, Santavuori Santavuori-Haltia disease; Vesa *et al.* 1995; Hellsten *et al.* 1996), classical late infantile NCL (LINCL; defective gene is CLN2; Jansky-Bielschowsky disease; Sleat *et al.* 1997), juvenile NCL (JNCL; defective gene is CLN3; Spielmeyer-Vogt-Sjögren disease; International Batten Disease Consortium 1995), adult NCL (Kuf's disease; defective gene is CLN4; Martin 1991), three variant forms of LINCL (defective genes are CLN5; Finnish variant; Savukoski *et al.* 1998), CLN6, Costa Rican variant (Gao *et al.* 2002; Wheeler *et al.* 2002) and CLN7, Turkish variant (Wheeler *et al.* 1999; Mitchell *et al.* 2001), a variant of JNCL (defective gene is CLN8; EPMR/NR; Ranta *et al.* 1999).

NCLs other than INCL are characterized by the accumulation of autofluorescent pigments containing mitochondrial ATP synthase subunit c (Palmer *et al.* 1989; Fearnley *et al.*

Received April 22, 2003; revised manuscript received July 31, 2003; accepted September 14, 2003.

Address correspondence and reprint requests to Eiki Kominami, Department of Biochemistry, Juntendo University School of Medicine, Hongo 2-1-1, Bunkyo-ku. Tokyo 113, Japan.
E-mail: kominami@med.juntendo.ac.jp

Abbreviations used: Cln3p, *CLN3* protein; LC-MS, liquid chromatography-mass spectrometry; ML, fraction, mitochondrial-lysosomal fraction; MS/MS, tandem MS spectrum; NCL, neuronal ceroid lipofuscinosis; PAGE, polyacrylamide gel electrophoresis; PNGase, F, peptide:N-glycosidase F; PVDF, polyvinylidene difluoride; SDS, sodium dodecyl sulfate; TCA, trichloroacetic acid; TOF, time of flight.

1990; Hall *et al.* 1991; Kominami *et al.* 1992; Ezaki *et al.* 1995). JNCL is the most common form of NCL. The *CLN3* gene was positionally cloned in 1995, and the gene product was predicted to be a novel 438 amino acid protein of unknown function. Northern blot analysis revealed the ubiquitous distribution of this protein (International Batten Disease Consortium 1995; Janes *et al.* 1996). Analysis of the predicted amino acid sequence suggested that Cln3p is a very hydrophobic integral membrane protein (type IIIb) containing six putative transmembrane domains, with four potential N-linked glycosylation sites and two putative O-glycosylation sites. The hydrophobicity of Cln3p was ascertained by an experiment in which GFP was conjugated to Cln3p using Triton X-114. Golabek *et al.* (1999) also suggested that the GFP tagged Cln3p was modified to a glycosylated form. The subcellular localization of Cln3p was mainly examined using cultured cells transfected with tagged or non-tagged Cln3p. Some groups claimed the presence of Cln3p in lysosomes and possibly also in late endosomes, and reported the co-localization of Cln3p with lysosomal marker proteins (Järvelä *et al.* 1998; Golabek *et al.* 1999; Haskell *et al.* 2000). However, another localization study revealed that Cln3p associates with nuclei and cell membranes (Margraf *et al.* 1999), Golgi apparatus (Kremmidiotis *et al.* 1999), and mitochondria (Katz *et al.* 1997). To resolve this issue, we have examined the localization of endogenous Cln3p in tissues. Several reports have demonstrated the existence of high amounts of Cln3p in brain (Margraf *et al.* 1999; Luiro *et al.* 2001); however, we could not confirm this tendency in rodent tissues. It is thought to be difficult to detect small quantities of an authentic protein using antibodies against synthetic peptides corresponding to partial sequences of the protein. In this study, we prepared two highly sensitive antibodies: one raised against peptides corresponding to an amino terminal sequence (residues 5–19) and the other raised against an internal sequence (residues 225–280) of mCln3p. The specificity of these antibodies was ascertained by their reactivity with expressed Cln3p and aminoacid sequencing of immunopurified Cln3p. Using these antibodies, we determined the distribution of Cln3p in rodent tissues and elucidated the intracellular localization of Cln3p.

Materials and methods

Materials

Percoll was obtained from Amersham Pharmacia Biotech Ltd (Uppsala, Sweden). Nylon membranes (GVHP) were from Nihon Millipore Ltd (Tokyo, Japan). Antibodies against synthetic peptides corresponding to the Cln3p sequences of the amino terminal regions (residues 5–19) and lgp110 (residues 410–411) were produced in rabbits as described by Liu *et al.* (1979). Polyclonal antibodies against rat cathepsin B, lgp120 were produced in rabbits as described by Kominami *et al.* (1992). Antibodies were purified by immunoaffinity chromatography using antigen-bound Sepharose 4B prior to use. Other antibody sources were as follows: monoclonal antibody against lysobisphosphatidic acid [LBPA; a epst from T. Kobayashi (Kobayashi *et al.* 1998)]; polyclonal antibodies against lgp85 and acid phosphatase [ACP; epsts from M. Himeno, Kyushu University (Himeno *et al.* 1988; Okazaki *et al.* 1992)]; polyclonal antibody against subunit IV of cytochrome oxidase (a epst from Y. Takamiya, Juntendo University; Takamiya *et al.* 1986)); monoclonal antibody against the Golgi 58 kDa protein (G58K; Sigma, St Louis, MO, USA); monoclonal antibodies against EEA1 and GM130 (BD Biosciences, Lexington, KY, USA); monoclonal antibody against protein disulfide isomerase, PDI (Daiichi Fine Chemicals, Toyama, Japan); monoclonal antibody against the 6xHis-probe and FLAG tag (Clontech, San Diego, CA, USA); monoclonal antibody against FLAG tag (Santa Cruz Biotechnology, Santa Cruz, CA, USA). Fluorescence second antibodies were Alexa Flour(R) 488-conjugated donkey anti-rabbit, Alexa Flour(R) 594-conjugated donkey anti-goat, Alexa Flour(R) 488-conjugated goat anti-rabbit and Alexa Flour(R) 594-conjugated goat anti-mouse (Molecular Probes Inc., Eugene, OR, USA).

Recombinant DNA

All procedures for recombinant DNA were carried out with *Escherichia coli* strain DH5a grown in Luria Broth medium with appropriate antibiotics. Molecular biological techniques were described by Ausubel *et al.* (1995). The pGEX4T-1 vector was purchased from Amersham-Pharmacia (Piscataway, NJ, USA), the pThioHisA vector was from Invitrogen (Carlsbad, CA, USA), and the pGem-T vector was from Promega (Madison, WI, USA). DNA sequencing was performed with a DNA sequencer 370 A (ABI).

Cloning of mouse CLN3 cDNA and plasmid construction

The mCLN3 cDNA was cloned by PCR amplification of a mouse brain cDNA library (Marathon). The mCLN3F primer (5′-ATGGGAAGTTCTGCGGGCTCGTGGAGGCGCC-3′, sense) and mCLN3R primer (5′- TCAAGGGAGGTGACAGAGGAAGT-CATGCAG-3′, antisense) were synthesized according to the sequence of GenBank accession number Q61124. Thirty cycles of amplification (denaturing at 94°C for 15 s, annealing at 55°C for 30 s, extension at 74°C for 90 s) produced a product of about 1.3 kilobases. This product was cloned into pGem-T (Promega) to make a plasmid, pmCLN3-GemT. To determine the sequence of this cDNA, three independent clones were isolated and sequenced.

To express FLAG-mCln3p in HEK293 cells, an *Eco*RI–*Sal*I site was introduced into pCMV-Tag2B vector (Stratagene, La Jolla, CA, USA) and designated pTag2BmCLN3. To express untagged mCln3p in HEK293 cells, an *Eco*RI–*Not*I site was introduced into pcDNA3 vector (Invitrogen) and designated pcDNA3mCLN3. To express 6xHis-mCln3p (containing enterokinase cleavage site) in HEK293 cells, an *Eco*RI–*Not*I site was introduced into pcDNA3.1/HisC vector (Invitrogen) and designated pcDNA3.1/HisCmCLN3.

Construction of Anti-CLN3 gene product (225–280 amino acid)

To construct an antibody against the mouse CLN3 gene product, we expressed a partial region (residues 225–280). The CLN3 sense primer (5′-GCCAGCTATTTCTTGTTGCTCAC-3′) and CLN3 antisense primer (5′-CTTGAACACTGTCCACCTTTCCTG-3′) were synthesized by ESPEC oligoservice (Tsukuba, Japan). Twenty cycles of amplification of pCLN3-GemT with the primers produced

a product of about 0.17 kilobases. The product was digested with *Bam*HI and *Sal*I, and introduced into the *Bam*HI–*Sal*I site of the pGEX4T-1 and pThioHisA vectors to make plasmids, pGST-CLN3 and pThio-CLN3, respectively. The plasmids were transformed into *E. coli* strain DH5a. Protein expression was carried out as recommended by the manufacturer (Amersham-Pharmacia). Protein in inclusion bodies was extracted with extraction buffer (6 M urea, 10 mM Tris–Cl, pH 9.5), separated by sodium dodecyl sulfate polyacrylamide gel electrophoresis (SDS–PAGE), and excised from the gel. Japanese white rabbits were immunized with the CLN3 antigens. Anti GST-fusion protein serum was purified on a thioredoxin-fusion protein column.

Expression of mCln3p in HEK293 cells

HEK293 cells were maintained in Dulbecco's modified Eagle's medium containing 10% fetal calf serum. For transfection, 2×10^5 cells were seeded in 60-mm dishes. After incubation for 24 h at 37°C, the cells were transfected with a mixture of 1 μg of plasmid DNA and 15 μL of Lipofectamine 2000. The transfectant was harvested after incubation for an additional 48 h. Cells were washed twice in ice-cold 0.25 M sucrose (pH 6.8) and homogenized in the same solution with 10 strokes of a glass homogenizer (Dounce, loose). The homogenate was centrifuged at 1000 *g* for 2 min to remove nuclei and unbroken cells. The unbroken cells were resuspended in 0.25 M sucrose and the homogenization cycle was repeated. The combined post-nuclear supernatant was centrifuged at 11 000 *g* for 20 min, and the precipitate was used as the mitochondrial–lysosomal fraction (ML fraction). The supernatant was further centrifuged at 105 000 *g* for 60 min, and the precipitate was used as the microsomal fraction.

Subcellular fractionation of liver

Highly purified lysosomes were obtained from the livers of dextran-injected rats by Percoll density gradient centrifugation as described by Ueno *et al.* (1991). ER fractions were obtained from the post-ML fractions by centrifugation at 60 min. Golgi fractions were prepared from rats according to the procedure of Howell and Palade (1982). Rat brains were prepared by the following procedures. Twenty percent of homogenates were prepared in 0.32 M sucrose with a Potter homogenizer. The homogenate was centrifuged at 650 *g* for 10 min, and the pellet was resuspended in the same volume of 0.32 M sucrose and recentrifuged. The supernatants from these two centrifugations were combined and centrifuged at 12 000 *g* for 20 min. We thus obtained ML fractions of rat brain.

Immunopurification of Cln3p

To analyze the amino acid sequence, Cln3p was immunopurified by affinity chromatography using anti –mCln3p (225–280) IgG-conjugated Sepharose 4B. We used rat liver instead of mouse liver to ensure a sufficient quantity of lysosomal membranes. Rat liver lysosomal membranes were purified according to the method of Ohsumi *et al.* (1983), and solubilized in 50 mM sodium phosphate buffer (pH 7.0) containing 1% NP-40. The extract was charged on a column packed with anti-mCln3p (225–280) IgG-conjugated Sepharose, and the column was washed with 50 mM sodium phosphate buffer (pH 7.0) containing 0.1% NP-40 and 0.2 M sodium chloride. Then, the column was eluted with 0.2 M glycine-HCl buffer (pH 2.4).

N-terminal sequence analysis

Immunopurified proteins were separated on 10% SDS–PAGE for N-terminal sequence analysis and mass spectrometric analysis by the method of Mineki *et al.* (2002). The N-terminal amino acid sequence of Cln3p on the polyvinylidene difluoride (PVDF) membrane of SDS–PAGE was determined by automated Edman degradation using an Applied Biosystems Model Procise cLC492 (Foster City, CA, USA) protein sequencer attached to an ABI 140D microgradient delivery system as a PTH amino acid analyer. The program was a modified routine 3.1.

Mass spectrometric analysis to identify proteins

The gel pieces of the protein bands were excised with a razor blade, destained with 100 mM ammonium carbonate-50% acetonitrile (several times), and digested with trypsin at 37°C for 16 h. The mixture of tryptic peptides were extracted with: (i) 50% acetonitrile containing 0.1%TFA; (ii) a mixture of isopropanol : formic acid : acetonitrile : purified water (15 : 20 : 25 : 40 v/v); and (iii) 80% acetonitrile. Those were loaded on a μLC-MS to identify protein. Peptide mapping was carried out using the API QSTAR Pulsar *i* hybrid mass spectrometer systems, which comprise nano-electrospray (nano-ESI) and time of flight (TOF; Applied Biosystems). The QSTAR hybrid mass spectrometer was combined with a micro liquid chromatograph (Magic 2002, Michrom Bioresources, Inc., Auburn, CA, USA) with an attached 0.2 mm ID × 50 mm Magic C18 column. The solvent system consisted of (A) 0.1% formic acid, and (B) 0.1% formic acid/90% acetonitrile. The solvent program was 5% B for 5 min, gradient at 1% B/min for 45 min and 100% B for 5 min The flow rate was 2.5 μL/min. The conditions for MS were as follows: ion spray voltage 3.8 kV; voltage for electron multiplier (CEM) 2200 V; and curtain gas nitrogen at 10 psi. Identification of proteins was performed using PROWL (ProFound) and public domain databases (NCBI) available on the Internet.

Proteinase K treatment

HEK293 cells were transfected with FLAG-tagged or untagged mCln3p. Freshly isolated ML fractions from transfected HEK293 cells were incubated on ice in medium (100 μL) containing 10 mM Tris–HCl (pH 6.8), 0.25 M sucrose, and Proteinase K (50 μg/mL) in the presence or absence of 1% Triton X-100. The reactions were stopped by adding 1 mL of 10% trichloroacetic acid (TCA). The pellets were collected by centrifugation at 5000 *g* for 10 min.

Enterokinase treatment

HEK293 cells were transfected with 6xHis tagged mCln3p. Freshly isolated ML fractions from transfected HEK293 cells were incubated with the indicated concentrations of enterokinase in 0.15 M NaCl containing 20 mM Tris–HCl (6.8) at 37°C for 4 h. After incubation, the samples were immediately solubilized in SDS treatment buffer.

Extraction of integral membrane proteins

Aliquots of organelles were suspended in 1.0 mL of distilled water and homogenized with a syringe (23G). The homogenates were centrifuged at 100 000 *g* for 1 h. The precipitates were suspended in 0.2 M Na_2CO_3 and homogenized with the syringe. The homogenates were centrifuged and the supernatants were removed as peripheral proteins. This procedure was repeated and the resulting pellets were

suspended in 1% Triton X-100. The homogenates were centrifuged at 100 000 *g* for 1 h. The extracted proteins were precipitated by adding 0.1 mL of 100% TCA. The pellets were collected by centrifugation at 5000 *g* for 10 min.

Analytical methods

Protein concentration was determined by BCA protein assay following the manufacturer's protocol (Pierce, Rockford, IL, USA). Proteins were analyzed by SDS–PAGE according to the method of (Laemmli 1970). Immunoblot analyses were performed by the ECL immunoblotting protocol (Amersham International, Buckinghamshire, UK) or the method of Towbin *et al.* (1979), except that an ECL detection kit was used as the substrate for the horseradish peroxidase conjugate of anti-rabbit IgG (Kobayashi and Tashima 1989). Samples were separated by SDS–PAGE and transferred to a nitrocellulose sheet (Towbin *et al.* 1979). The nitrocellulose sheet was soaked in Tris-buffered saline (10 mM Tris, pH 8.0, 150 mM NaCl) containing 5% skim milk for 1 h at room temperature, and then incubated at room temperature for 2 h with various affinity-purified IgGs (5 μg/mL in Tris-buffered saline containing 1% bovine serum albumin). The nitrocellulose sheet was washed five times with Tris-buffered saline containing 0.05% Tween-20.

Biochemical assays

Fluorometric assays for cathepsin B plus L (Barrett and Kirschke 1981) and cathepsin D (Yasuda *et al.* 1999) were carried out using benzoyl-Phe-Ala-arginyl-4-methyl-coumaryl-7-amide and MOCAc-Gly-Lys-Pro-Ile-Ile-Phe-Phe-Arg-Leu-Lys(Dnp)γ-NH_2, respectively, as substrates. Glucose-6-phosphate was assayed by the colourometric measurement of released Pi (Morre 1971). Succinate-INT reductase was assayed according to the method of Morre (1971). SDS–PAGE was carried out by the method of Laemmli (1970). Immunoblot analysis was carried out by the method of Towbin *et al.* (1979).

Immunofluorescence microscopy

Immunofluorescence microscopic analysis was performed according to the method of Koike *et al.* (2002). Briefly, rat liver was fixed with 4% paraformaldehyde buffered with 0.1 M phosphate buffer, pH 7.2, containing 4% sucrose. The tissues were processed for paraffin embedding, cut at 5 μm with a microtome, and placed on silane-coated glass slides. Deparaffinized sections were incubated with a mixture of anti-mCln3 IgG (5–19) and the different IgGs against markers of organelles at 4°C for 24 h, followed by detection with second antibodies using donkey anti-rabbit IgG coupled with Arexa 488 for Cln3p, donkey anti-goat IgG coupled with Arexa 594 for acid phosphatase (Fig. 4A), goat anti-rabbit IgG coupled with Arexa 488 for Cln3p, and goat anti-mouse IgG coupled with Arexa 594 for other markers of organelles (Fig. 4B). Specimen were niewed with confocal laser scan micropscope (Olympus, LSM-GB200).

Results

Expression of Cln3p in HEK293 cells

To study the properties and cellular distribution of Cln3p, we prepared two kinds of antibodies against mouse Cln3p (mCln3p). One was generated against peptides corresponding to the amino terminal region of mCln3p [residues 5–19, hereafter denoted anti-mCln3p (5–19) antibody] and the other was generated against the glutathione s-transferase (GST) fusion protein fused to the peptide corresponding to the central portion of mCln3p [residues 225–280, hereafter denoted anti-mCln3p (225–280) antibody]. First, we verified the specificity of these antibodies by immunoblotting analysis to expressed mCln3p. HEK293 cells were transiently transfected with mouse *CLN3* cDNA constructs expressing FLAG-tagged and untagged mCln3p. The cells were homogenized and fractionated into micrososmal and ML fractions by differential centrifugation. Each fraction was subjected to SDS–PAGE and then to immunoblotting analysis. As shown in Fig. 1(a), both FLAG-tagged and untagged mCln3p were detected mainly in the ML fractions by the anti-mCln3p (5–19) antibody. Expressed untagged mCln3p showed a major band with an apparent molecular mass of 60 kDa, with a number of minor bands between 45 kDa and 66 kDa also detected. FLAG-tagged mCln3p was also recovered in the ML fractions; the major band migrated with an apparent molecular mass of 62 kDa accompanied by minor bands, the same as for untagged mCln3p. The small difference in mobility can be attributed to the size difference between FLAG-tagged and untagged mCln3p (about 2.5 kDa). These signals for FLAG-tagged and untagged mCln3p were abolished by pre-absorption with the peptide corresponding to the amino terminal region of mCln3p (residues 5–19; Fig. 1c). FLAG-mCln3p in the ML fraction was also recognized by the anti-FLAG antibody (Fig. 1b). Therefore, the anti-mCln3p (5–19) antibody was confirmed to recognize expressed mCln3p specifically. The anti-mCln3p (225–280) antibody also recognized mCln3p (Fig. 1d). Neither of the two antibodies recognized human Cln3p expressed in HEK293 cells (data not shown).

Expressed mouse Cln3p contains N-linked oligosaccharides

Based on the primary amino acid sequence, Cln3p comprises four putative N-glycosylation sites. As described above, the expressed untagged mCln3p has a major 60 kDa band and minor heterogeneous bands of about 45–66 kDa. It is likely that these bands are caused by heterogeneous glycosylation. In order to examine whether expressed mCln3p undergoes post-translational glycosylation, expressed FLAG-tagged and untagged mCln3p in cell lysates was treated with peptide: N-glycosidase F (PNGase F). PNGase F is an enzyme that releases N-linked oligosaccharides from polypeptides completely. The resulting samples were analyzed by immunoblotting analysis. After PNGase F treatment, the heterogeneous bands of expressed untagged mCln3p shifted to 45 and 42 kDa bands. In the case of FLAG-tagged mCln3p, the apparent molecular masses of the deglycosidated forms shifted to 47 and 44 kDa (Fig. 1e).

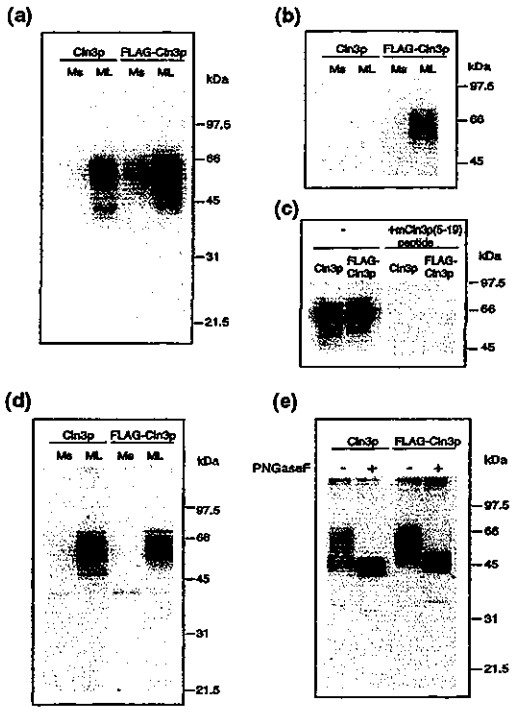

Fig. 1 Immunoblot analysis of expressed Cln3p in HEK293 cells. FLAG-tagged and untagged mCln3p were expressed in HEK293 cells. Cells were homogenized and fractionated into microsomal fractions (Ms) and mitochondrial-lysosomal fractions (ML) (a, b, and d). Expressed proteins were detected with anti-mCln3p (5–19) antibody (a, c and e), anti-FLAG antibody (b), and anti-mCln3p (225–280) antibody (d). The signals for FLAG-tagged and untagged mCln3p detected by anti-mClp3p (5–19) antibody were abolished by preabsorption with the peptide corresponding to the amino terminal region of mCln3p (residues 5–19) (c). The deglycosidated form of Cln3p was obtained by treatment with N-glycosidase F (PNGase F) (e).

The sizes of the deglycosidated products are consistent with those predicted from the amino acid composition of mCln3p. Unexpectedly, both FLAG-tagged and untagged mCln3p treated with PNGase F showed two bands. It has been reported that Cln3p has two putative O-glycosylation sites (Janes *et al.* 1996). The lower molecular weight protein may lack modification by O-linked oligosaccharides after translation due to the overexpression (Fig. 1e).

Investigation of Cln3p in rodents tissues

To investigate the endogenous mCln3p, we used whole homogenates of mice organs. We removed peripheral membrane proteins with 0.2 M Na_2CO_3 and extracted the integral membrane proteins with 1% Triton X-100. The extracts were then precipitated with 10% TCA to concentrate the proteins, and the precipitates were examined by immunoblotting analysis using the anti-mCln3p (5–19) antibody. As shown in Fig. 2(a), lgp120 and lgp85 signals were strongly detected in all organs tested, although the lgp110 signal was faint in brain and spleen. These results are consistent with the results of Andrejewski *et al.* (1999). A shift in the molecular size of brain lgp120 has also been reported by the same authors (Andrejewski *et al.* 1999). Using the same samples, mCln3p was detected in liver, kidney and spleen as a broad band between 45 kDa and 66 kDa, while mCln3p in the brain and pancreas was scarcely detected. In light of the importance of Cln3p in the symptoms and progression of JNCL, it is necessary to characterize Cln3p in neuronal tissues. However, we could not detect mCln3p in the brain by ordinary immunoblotting analysis after detergent extraction. This is probably because the content of Cln3p in brain is very small.

To detect a small quantity of Cln3p without disturbance by impurities, we purified Cln3p from several mouse organs by affinity chromatography using anti-mCln3p (225–280) IgG-conjugated Sepharose. Mouse organs were extracted with 50 mM sodium phosphate buffer (pH 7.0) containing 0.5% NP-40, 0.05% SDS and 0.15 M NaCl, and the extracts were charged on an anti-mCln3p (225–280) IgG-conjugated Sepharose column. The column was washed with 50 mM sodium phosphate buffer (pH 7.0) containing 0.1% NP-40 and 0.2 M NaCl. mCln3p was eluted with 0.1 M glycine HCl buffer (pH 2.8) containing 0.1% NP-40. The samples obtained were analyzed by immunoblotting using the anti-mCln3p (5–19) antibody. As shown in Figs 2(b and c), mCln3p was specifically obtained from all organs including brain of mice. Almost same results were obtained by using either anti-mCln3p (5–19) IgG (Fig. 2b) or anti-mCln3p (225–280) IgG conjugated Sepharose (Fig. 2c). The amount of brain Cln3p was much lower than that of liver Cln3p. The size of brain Cln3p was about 55 kDa, slightly smaller than its liver counterpart. The difference in molecular masses between these mCln3p molecules may be attributable to a differential rate of glycosylation. The liver and brain Cln3p showed mobility shifts to 45 kDa after PNGase F treatment, however, Endo H treatment had no effect on the mobility of liver or brain mCln3p (Fig. 2d). These findings indicate that both liver and brain mCln3p possess complex-type N-linked sugar chains. mCln3p was detected as a single band by immunoblotting analysis using anti-mCln3p (5–19) IgG.

Subcellular localization of endogenous Cln3p

To analyze the endogenous mCln3p distribution in cells, we carried out subcellular fractionation of mouse liver using a Percoll density gradient. In this experiment, the post-nuclear supernatant was divided into microsomal, mitochondrial, lysosomal content, and lysosomal membrane fractions (Fig. 3a, Table 1). Each sample was analyzed by immunoblotting analysis using anti-mCln3p (5–19) IgG. As shown in Fig. 3(a), the anti-mCln3p (5–19) antibody recognized a sharp band with an apparent molecular mass of 50 kDa in the mitochondrial fraction (asterisk in Fig. 3a) and a soft-focused

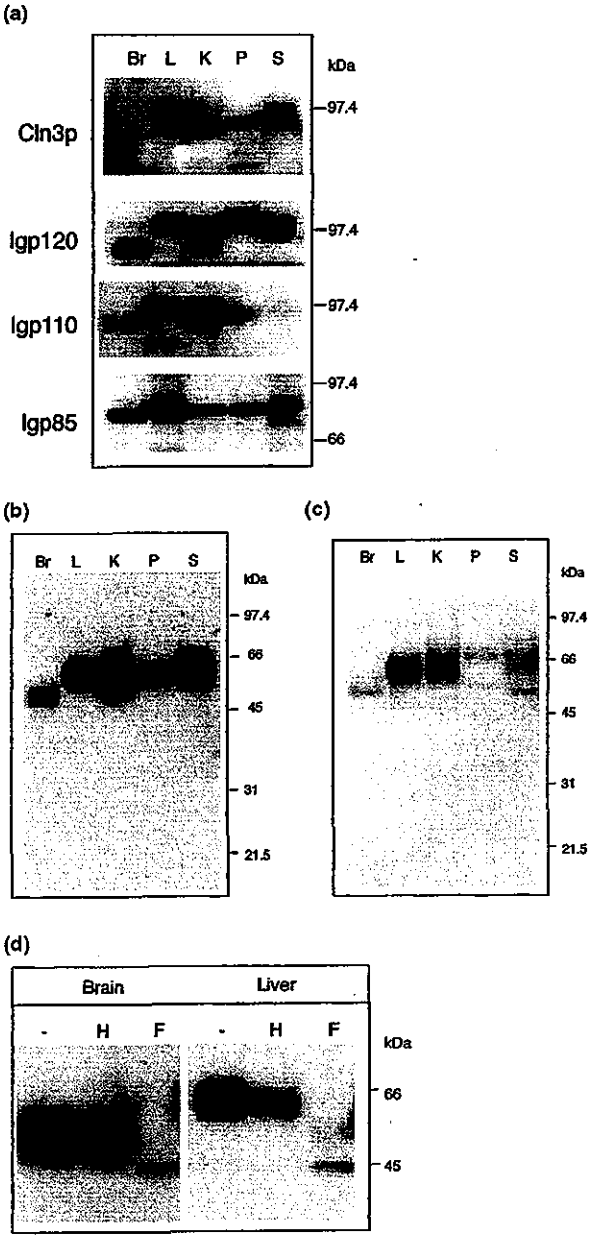

Fig. 2 Comparative examination of mCln3p in mouse tissues. (a) Aliquots of mouse brain (Br), liver (L), kidney (K), pancreas (P), and spleen (S) were treated with 0.2 M Na_2CO_3 to remove loosely bound peripheral membrane proteins and centrifuged. Subsequently, the precipitates were extracted with 1% Triton X-100 and analyzed by immunoblotting. mCln3p and lysosomal membrane proteins were detected using anti-mCln3p (5–19), Igp120, Igp110, and Igp85 antibodies. (b and c) mCln3p of mouse tissues was immunopurified from the ML fractions as described in the text, using anti-mCln3p (225–280) IgG-conjugated Sepharose 4B (b) or anti-mCln3p (5–19) IgG conjugated Sepharose 4B (c). The immunopurified proteins were subjected to 10% SDS–PAGE and examined by immunoblotting analysis using anti-mCln3p (5–19) antibody. (d) Immunopurified proteins of brain and liver were treated with Endo H (H) or PNGase F (F) according to the BioLabs protocol. The samples obtained were subjected to 10% SDS–PAGE and examined by immunoblotting using anti-mCln3p (5–19) antibody.

band with an apparent molecular mass of 60 kDa in the lysosomal membrane fraction. The immunoreactivity of the mitochondrial 50 kDa polypeptide was thought to be false positive because this polypeptide was completely stripped from mitochondria by treatment with 0.2 M Na_2CO_3 (not shown), a characteristic of peripheral proteins associated with the membrane surface. As mCln3p is predicted to be a very hydrophobic integral membrane protein, authentic mCln3p would not be solubilized by this alkaline treatment. Furthermore, this 50 kDa molecule was not detected by anti-mCln3p(225–280) IgG (Fig. 3b) and was not adsorbed on anti-mCln3p (5–19) Sepharose (described above). In contrast, the 60 kDa lysosomal membrane protein was not stripped by treatment with 0.2 M Na_2CO_3 and was also detected by the anti-mCln3p (225–280) antibody (Fig. 3b). In another experiment, the 60 kDa protein was ascertained to be authentic mCln3p by determination of the amino acid sequence of the 60 kDa protein immunopurified from lysosomal membranes using anti-mCln3p (225–280) IgG-conjugated Sepharose (described below).

The localization of Cln3p on Golgi apparatus or ER has also been claimed. To investigate these possibilities, we fractionated Golgi apparatus and ER from rat liver by the method of Palade. As shown in Fig. 3(c), Cln3p was not detected in the Golgi or ER fractions. From these results, we conclude that Cln3p specifically localizes in lysosomal membranes.

Next, to analyze the subcellular distribution of endogenous Cln3p morphologically, we carried out immunofluorescence microscopic analysis of rat liver stained for Cln3p and several markers of subcellular compartments (Figs 4a and b). Positive staining of Cln3p was detected in the liver. Dotted immunoreactivity for Cln3p was seen in hepatocytes (Fig. 4a). Partial overlapping was detected for Cln3p and the lysosomal marker acid phosphatase (ACP). Cln3p-immunoreactive granule were also partially co-labeled with LBPA (a late endosomal marker), but not with a EEA1 (an early endosomal marker), GM130 (a *cis*-Golgi marker), and PDI (an ER marker; Fig. 4b). Kupffer cells showed intense immunorectivity for Cln3p (Fig. 4a), and the best co-localization with ACP was observed at the edges of the cells. These observations also indicate that Cln3p primarily localizes in lysosomes/late endosomes.

Identification of Cln3p by mass spectrometry

Our results show that Cln3p abundantly existed in the liver, kidney and spleen, and has an apparent molecular mass of

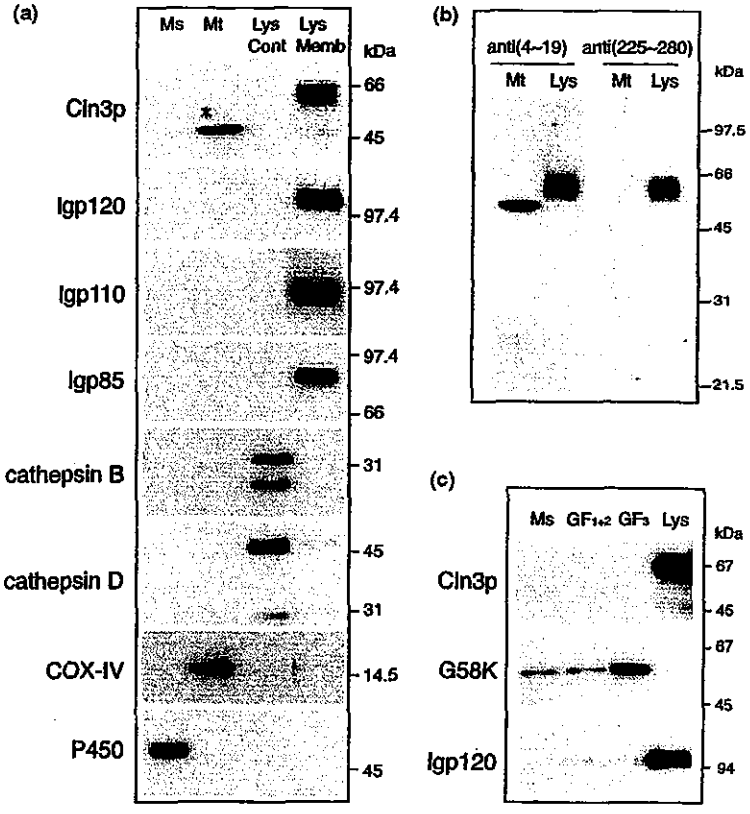

Fig. 3 Endogenous Cln3p distribution in mouse liver. (a) Microsomal fractions (Ms) were obtained from the post-ML fractions of livers of dextran-injected mice by centrifugation at 105 000 *g* for 60 min. Mitochondrial fractions (Mt), lysosomal content (Lys Cont), and lysosomal membranes (Lys Memb) were separated on a Percoll density gradient centrifugation as described by Ueno *et al.* (1991). These fractionated samples were analyzed by immunoblotting using anti-mCln3p (5–19), anti-Igp120, anti-Igp110, anti-Igp85. Anticathepsin B, anticathepsin D, antisubunit IV of cytochrome oxidase (COX-IV), and anticytochrome P450 (P450) antibodies. (b) Samples of mitochondrial fractions (Mt) and lysosomal fractions (Lys) were analyzed by immunoblotting using anti-mCln3p (5–19) antibody, anti-mCln3p (225–280) antibody (c) Golgi and ER fractions were prepared by the method of Howell and Palade (1982). Golgi fractions were divided into light and intermediate Golgi fraction (GF1+2) and heavy Golgi fraction (GF3) by its gravity. These fractionated samples were analyzed by immunoblotting using anti-mCln3p (5–19), -Golgi 58 kDa (G58K), and -Igp120 antibodies. Equal amounts of samples (10 μg) were separated on 10% SDS–PAGE for Cln3p, Igp120, and G58K or 16.5% Tricine–SDS–PAGE for COX-IV (a and b).

Table 1 Marker enzyme activities of divided fraction

	Microsomal fraction	Mitochondrial fraction	Lysosomal fraction	Lysosomal content (nmole/mg protein)
Cathepsin B plus L	4.99 ± 0.11	0.438 ± 0.053	10.33 ± 0.41	23.42 ± 3.38
Cathepsin D	0.552 ± 0.01	0.123 ± 0.025	66.2 ± 1.25	88.54 ± 4.30
Succinate:INT reductase	3.23 ± 0.208	134.0 ± 7.2	1.5 ± 2.6	0.4 ± 0.69
Glucose-6-phosphatase	434.3 ± 17.5	111.3 ± 5.1	180.3 ± 16.7	79.7 ± 2.3

Marker enzyme activities for lysosomes (cathepsin B plus L), mitochondria (succinate:INT reductase), and microsomes (glucose 6-phosphatase) were determined as described in Materials and methods. Means with standard deviations for the results of three experiments are shown.

about 60 kDa. Unexpectedly, we could not detect a strong Cln3p signal in the lysosomal fractions of mouse brain. Our results are contradictory to those of previous reports (Margraf *et al.* 1999; Luiro *et al.* 2001). To ensure the reliability of our results, the product immunopurified from the lysosomal membrane by affinity chromatography using anti-mCln3p IgG was confirmed by liquid chromatography-mass spectrometry (LC-MS) to be Cln3p. Proteins were

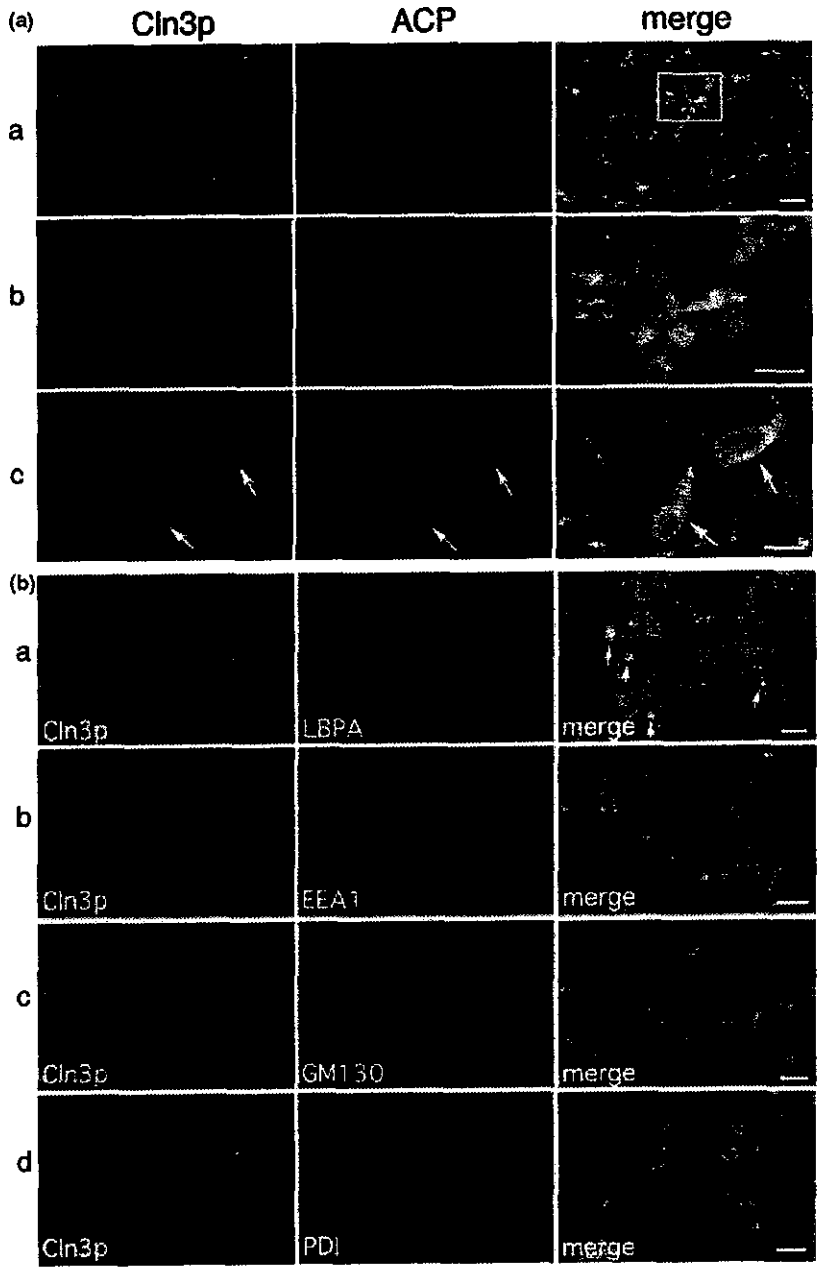

Fig. 4 Localization of endogenous Cln3p in rat liver. (a) Double immunostaining of liver section with anti-mCln3p (5–19) antibody (green colour) and antiacid phosphatase (ACP) antibody, a lysosomal marker (red colour). An overlaid figure shows that a part of the Cln3p immunoreactivity is detected in ACP-positive granules in the hepatocytes (i and ii). Kupffer cells (iii) were strongly stained by anti-mCln3p IgG and colocalization with ACP was observed at the edges of the cells. Arrows indicate examples of co-localized vesicles. Scale 10 μm (i, iii), 5 μm (ii). (b). Double immunostaining of Cln3p (green colour) and different organelles markers (red colour) was carried out with anti-LBPA for a late endosomal marker, anti-EEA1 for early endosomal marker, anti-GM130 for a *cis*-Golgi marker and anti-PDI for an endoplasmic reticulum marker. Arrows indicate examples of co-localized vesicles. Scale 10 μm.

separated by SDS–PAGE according to the method of Mineki *et al.* (2002) yielding four bands at 63.0, 58.0, 53.5, and 51.3 kDa as shown in Fig. 5(a). Then, all bands were subjected to gel digestion for peptide mapping, and the tryptic peptides in each band were loaded onto the LC-MS (Mineki *et al.* 2002). Three tryptic peptides in band 3 were derived from Cln3p (*Fig. 5b*). The amino acid sequence of the peptide at 9.2 min was estimated to comprise residues 310–320 of Cln3p, 'NTSLSHAQQYR' (MW 1303.7), by the MS/MS mode (not shown). Also, the amino acid sequences of the peptides at 13.01 min and 19.22 min were residues 263–274 (MW 1357.8) and 113–127 (MW 1659.2) of Cln3p, respectively. These peptides were included in all bands even though the recoveries differed slightly in each band. This may be caused by the different rate of glycosylation of Cln3p.

The bands were also analyzed with a protein sequencer to confirm the NH_2 terminal amino acid sequence of Cln3p, but these were completely blocked. From these results, it is demonstrated that the immunopurified 60 kDa protein is undoubtedly rCln3p and our antibodies correctly recognize rodent Cln3p.

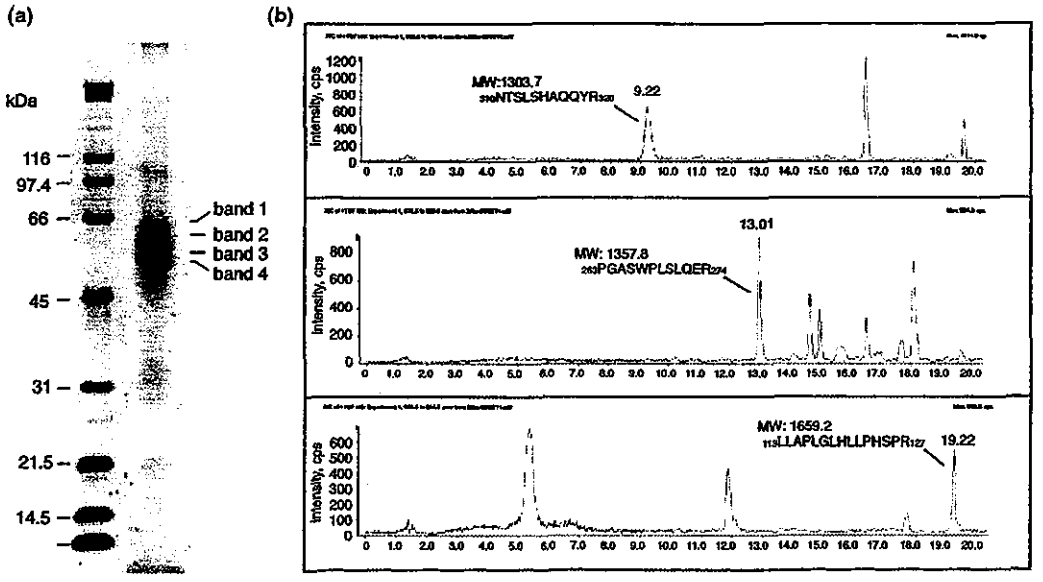

Fig. 5 Identification of Cln3p by mass chromatography. (a) Cln3p was immunopurified from rat liver lysosomes by using anti-Cln3p (225–280) IgG-conjugated Sepharose 4B. The purified protein was analyzed by 10% SDS–PAGE and stained with Coomasie Brilliant Blue. (b) The gel pieces of the protein bands were excised with a razor blade and digested with trypsin at 37°C for 16 h. The mixture of tryptic peptides were extracted and analyzed as described in Materials and methods. Three tryptic peptides of Cln3p were confirmed by the selected ion monitoring profiles at the $[M + 2H]2+$.ion (a) m/z 652.8, (b) m/z 677.9, and at the $[M + 3H]^{3+}$ ion (c) m/z 554.0.

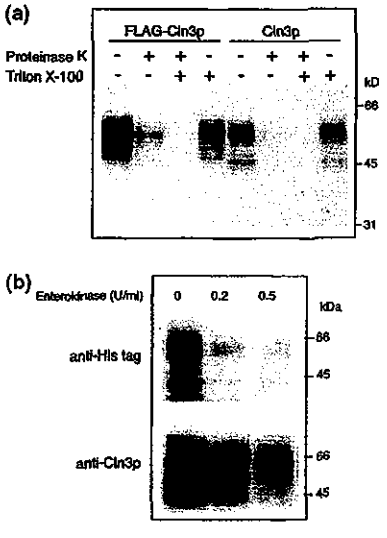

Fig. 6 Topology of Cln3p on lysosomal membranes. (a) ML fractions prepared from HEK293 cells expressing FLAG-tagged or untagged mCln3p were treated with proteinase K (50 μg/mL) for 30 min on ice in the presence or absence of 1% Triton X-100. The remaining immunoreactivity of the N-terminal region of Cln3p against anti-mCln3p (5–19) IgG was determined by immunoblot analysis. (b) ML fractions prepared from HEK293 cells expressing 6xHis-tagged mCln3p. The expressed protein contained an enterokinase cleavage site between the 6xHis-tag and amino-terminus of mCln3p.After enterokinase treatment, the remaining immunoreactivities against anti-His tag and mCln3p antibodies were determined by immunoblot analysis.

Topology of Cln3p on lysosomal membranes

As described above, the amino-terminal sequence of Cln3p could not be detected by direct sequence analysis by automated Edman degradation, suggesting that Cln3p has a blocked amino terminus. Furthermore, this protein was recognized by the antibody against mCln3p (5–19). From these results, it is predicted that the amino-terminus of Cln3p faces the cytosol and accepts post-translational modification as in the case of cytosolic proteins. To investigate this possibility, we examined the topology of Cln3p using untagged mCln3p, His-tagged mCln3p (containing an enterokinase cleavage site between the 6xHis tag and the amino terminus of mCln3p), and FLAG-tagged mCln3p expressed in HEK293 cells. First, we examined the susceptibility of the amino terminal region of mCln3p to protease treatment. ML fractions prepared from HEK293 cells expressing FLAG-tagged or untagged mCln3p were treated with proteinase K and analyzed for remaining immunoreactivity by immunoblotting analysis. If the amino terminal region of mCln3p faces the cytosol, then the amino terminal FLAG epitope of mCln3p will be sensitive to proteinase K treatment. As shown in Fig. 6(a), the amino-terminal FLAG epitope was digested immediately by proteinase K treatment even in the absence of Triton X-100.

Next we performed enterokinase treatment of ML fractions prepared from HEK293 cells expressing the 6xHis-tag at the amino-terminal of mCln3p. The expressed protein contained an enterokinase cleavage site between the 6xHis tag and the

amino terminal. 6xHis-tagged mCln3p was detected by immunoblotting analysis using anti6xHis tag or mCln3p (5–19) antibodies. After enterokinase treatment, the 6xHis-epitope of mCln3p disappeared completely even in the absence of detergent, whereas the remaining mCln3p with the deleted amino terminal 6xHis epitope was detected by the anti-mCln3p (5–19) antibody (Fig. 6b). From these results, it was concluded that the amino terminal region of mCln3p is not buried in the lysosomal membrane bilayer, but exposed to the cytosolic side.

Discussion

Preparing a specific antibody to Cln3p is very difficult due to its extreme hydrophobicity. In order to prepare useful antibodies to Cln3p, we took notice of two regions in Cln3p that are enriched with hydrophilic amino acids and, hence, thought to be exposed to the outer surface of the molecule. We prepared antibodies against the amino terminal region (residues 5–19) and the central region (residues 225–280) of mCln3p. The two antibodies showed high sensitivity to mCln3p expressed in HEK293 cells. Using these antibodies, we performed biochemical analyses of endogenous and expressed Cln3p.

Cln3p expressed in HEK293 cells showed apparent molecular masses between 45 and 65 kDa, apparently caused by the attachment of heterogeneous N-linked oligosaccharide chains. The molecular mass decreased to 45 kDa by PNGase F treatment. Similar results have been reported for the expressed GFP fusion protein of Cln3p (Golabek *et al.* 1999; Kremmidiotis *et al.* 1999). The apparent molecular mass of endogenous Cln3p was found to be about 60 kDa in liver, kidney, pancreus and spleen, and about 55 kDa in brain. This shift in the molecular weight is sometimes detected for lysosomal membrane proteins as described above (Fig. 2a) and by others (Andrejewski *et al.* 1999). In the liver, endogenous Cln3p was specifically detected in lysosomal membranes but not in ER or Golgi apparatus. The lysosomal Cln3p was not solubilized with 0.2 M Na_2CO_3 but was extracted with 1% Triton X-100. The Triton X100-solubilized Cln3p showed a molecular mass of around 60 kDa and was detected by both antibodies. Amino acid sequence analysis of the immunopurified 60 kDa molecule after in-gel digestion and mass spectrometry clearly matched the predicted sequence of Cln3p. This is the first report of the sequence determination of endogenous Cln3p. From these results, we conclude that the 60 kDa lysosomal membrane protein is genuine Cln3p. In previous reports, a Cln3p form of ~43 or ~44 kDa was detected by immunoblot analysis after over-expression experiments (Järvelä *et al.* 1998; Kremmidiotis *et al.* 1999; Cotman *et al.* 2002). We believe that the smaller molecules obtained in these experiments in contrast to our results are the result of incomplete oligosaccharide modification after overexpression in the cells, because these molecular sizes are almost the same as the size of endogenous Cln3p after PNGase F treatment (Fig. 2c). Our data also clearly rule out other candidates, such as 50 kDa and 45 kDa components reported in previous studies (Katz *et al.* 1997; Margraf *et al.* 1999; Luiro *et al.* 2001). Furthermore, anti Cln3p (5–19) IgG and anti Cln3p (225–280) IgG did not immunoprecipitate these non-specific molecules in the presence of non-ionic detergents. Taking advantage of this specificity, we could detect endogenous Cln3p by microscopic analysis. Endogenous Cln3p was observed as dot like structures in hepatocyte and kupffer cells. It was significantly co-localized with the lysosomal marker protein acid phosphatase and partially with late endosomal marker LBPA (Figs 4a and b). Signals for ER marker PDI, Golgi marker GM130 or early endosomal marker EEA1 were not overlapped with those for Cln3p (Figs 4a and b). These results and the data on subcellular fractionation (Figs 3a–c) indicate that Cln3p is primarily localized in lysosomes and partly in late endosomes in rodent liver.

It is surprising that the amount of Cln3p in brain is much lower than that in liver. Previous papers have reported the specific existence of Cln3p in brain, in particular, in synaptosomal fractions (Margraf *et al.* 1999; Luiro *et al.* 2001), and these results were not only acquired by immunoblotting analysis but also by immunochemical microscopic analysis. We took it for granted that brain contains large amounts of Cln3p, because NCL is a neurodegenerative disease; however, we detected only small quantities of Cln3p in cerebrum after immunopurification by antibody-conjugated Sepharose. Of course, the significance of Cln3p in the central nervous system is not changed by its small quantity.

The responses of brain Cln3p to PNGase F and Endo H treatment are similar to those of liver Cln3p. The molecular size of both brain and liver Cln3p converged to 45 kDa after PNGase F treatment, a value that coincides with the predicted molecular mass of the core Cln3p polypeptide without glycosylation (International Batten Disease Consortium 1995). The size of deglycosylated Cln3p was almost same as the size of overexpressed Cln3p (Järvelä *et al.* 1998; Kremmidiotis *et al.* 1999; Cotman *et al.* 2002) as described above. The apparent difference in molecular size between liver and brain Cln3p is caused by differential modification by oligosaccharide chains.

It is claimed that Cln3p is a type-IIIb membrane protein based on hydropathy calculation, i.e. it contains six putative transmembrane domains (International Batten Disease Consortium 1995; Janes *et al.* 1996). Our results suggest that the amino terminal region of mCln3p faces the cytosol for the following reasons:

1. The amino terminus of Cln3p is likely to be blocked and resistant to Edman degradation
2. The amino terminal region of untagged Cln3p and FLAG-Cln3p in lysosomal membranes is susceptible to protease digestion

3. The anti-Cln3p (5–19) antibody recognizes mature lysosomal Cln3p. This means that the amino terminal sequence of Cln3p is not cleaved post-translationally
4. The enterokinase cleavage site in the connective region between the His-tag and amino-terminus of Cln3p is susceptible to externally added enterokinase.

It is known that certain deletions or mutations of Cln3p cause the deposit of a subunit c of F_0F_1-ATP synthase. What is the role of Cln3p relevant to the degradation of subunit c? BTN1 may be an important clue as to the normal function of Cln3p. BTN1 is a yeast homologue of Cln3p and shows 39% identity and 59% similarity to human Cln3p (Pearce and Sherman 1997). The growth medium of a BTN1 deletion mutant of yeast undergoes an apparent decrease in pH due to the increased activity of plasma membrane H ± ATPase during the early phase of growth. This effect is abolished by the introduction of human *CLN3* (Pearce *et al.* 1999). From these results, Cln3p seems to act to regulate lysosomal pH and the Cln3p mutation may lead to an altered lysosomal pH. As we described before, the optimum pH for subunit c degradation is around pH 4.5, in accordance with the optimum pH of TPP-I (Ezaki *et al.* 1996, 2000). This means that a shift in lysosomal pH caused by a Cln3p abnormality may cause an accumulation of subunit c. Recently, Golabek *et al.* (2000) suggested that wild-type Cln3p increases lysosomal pH in HEK293 cells. Intracellular pH is also important for the transport of subcellular organelles and other physiological phenomena. In addition, Vesa *et al.* (2002) suggested that Cln5p interacts with TPP-I and Cln3p based on coimmunoprecipitation and *in vitro* binding assays. Cln3p may regulate the activity of TPP-I through the interaction with Cln5p.

Why does a defect in this protein cause a neurodegenerative disease? The accumulation of subunit c may cause a membranous abnormality in neurons due to unknown toxicity. The specific accumulation of proteins or other materials has also been detected in many kinds of lysosomal disease and sometimes is accompanied by neurodegeneration. However, as yet there is no proof of a relationship between the accumulation of subunit c and the neurodegeneration in NCL. It is necessary to examine the relationship between protein deposition and cell degeneration.

The investigation of endogenous Cln3p is significant for understanding the mechanism of NCL. This study provides a basis for analyzing the role ofCln3p in normal and disease cells. Further studies on the interaction between Cln3p and other CLN proteins will be required for further understanding of the molecular pathogenesis of NCLs.

Acknowledgements

We thank Drs I. Tanida, K. Ishidoh, D. Muno, and T. Nemoto (Juntendo University) for helpful discussion. We also thank Margaret Dooley-Ohto for editing the language of the manuscript. This work was supported, in part, by Grant-in-Aid 12470040 for Scientific Research, Grant-in-Aid 12146205 for Scientific Research on Priority Areas from the Ministry of Education, Science, and Culture of Japan and The Science Research Promotion Found Fund from the Japan Private School Promotion Foundation.

References

Andrejewski N., Punnonen E.-L., Guhde G., Tanaka Y., Lüllmann-Rauch R., Hartmann D., von Figura K. and Saftig P. (1999) Normal lysosomalmorphology and function in LAMP-1-deficient mice. *J. Biol. Chem.* **274**, 12692–12701.

Ausubel F., R. Brent R. E., Kingston D. D., Moore J. G., Seidman J. A., Smith and K. Struhl (1995) *Short protocols in molecular biology*, 3rd edn. John Wiley & Sons, Inc, Philadelphia.

Barrett A. J. and Kirschke H. (1981) Cathepsin B, cathepsin H, and cathepsin L. *Methods Enzymol.* **22**, 130–148.

Cotman S. L., Vrbanac V., Lebel L.-A. *et al.* (2002) $Cln3^{\Delta ex7/8}$ knock-in mice with the common JNCL mutation exhibit progressive neurologic disease that begins before birth. *Hum. Mol. Genet.* **11**, 2709–2721.

Ezaki J., Wolfe L. S., Higuti T., Ishidoh K. and Kominami E. (1995) Specific delay of degradation of mitochondrial ATP synthase subunit c in late infantile neuronal ceroid lipofuscinosis (Batten disease). *J. Neurochem.* **64**, 733–741.

Ezaki J., Wolfe L. S. and Kominami E. (1996) Specific delay in the degradation of mitochondrial ATP synthase subunit c in late infantile neuronal ceroid lipofuscinosis is derived from cellular proteolytic dysfunction rather than structural alteration of subunit c. *J. Neurochem.* **67**, 1677–1687.

Ezaki J., Takeda-Ezaki M., Oda K. and Kominami E. (2000) Characterization of endopeptidase activity of tripeptidyl peptidase-I/CLN2 protein which is deficient in classical late infantile neuronal ceroid lipofuscinosis. *Biochem. Biophys. Res. Comm.* **268**, 904–908.

Fearnley I. M., Walker J. E., Martinus R. D., Jolly R. D., Kirkland K. B., Shaw G. J. and Palmer D. N. (1990) The sequence of the major protein stored in ovine ceroid lipofuscinosis is identical with that of the dicyclohexylcarbodiimide-reactive proteolipid of mitochondrial ATP synthase. *Biochem. J.* **268**, 751–758.

Gao H., Boustany R.-M. N., Espinola J. A. *et al.* (2002) Mutations in a novel CLN6-encoded transmembrane protein cause variant neuronal ceroid lipofuscinosis in man and mouse. *Am. J. Hum. Genet.* **70**, 324–335.

Golabek A. A., Kaczmarski W., Kida E., Kaczmarski A., Michalewski M. P. and Wisniewski K. E. (1999) Expression studies of CLN3 protein (Battenin) in fusion with the green fluorescent protein in mammalian cells *in vitro*. *Mol. Genet. Met.* **66**, 277–282.

Golabek A. A., Kida E., Walus M., Kaczmarski W., Michalewski M. and Wisniewski K. E. (2000) CLN3 protein regulates lysosomal pH and alters intracellular processing of Alzheimer's amyloid-β protein precursor and cathepsin D in human cells. *Mol. Genet. Met.* **70**, 203–213.

Hall N. A., Lake B. D., Dewji N. N. and Patrick A. D. (1991) Lysosomal storage of subunit c of mitochondrial ATP synthase in Batten's disease (ceroid-lipofuscinosis). *Biochem. J.* **275**, 269–272.

Haskell R. E., Carr C. J., Pearce D. A., Bennett M. J. and Davidson B. L. (2000) Batten disease: evaluation of CLN3 mutations on protein localization and function. *Hum. Mol. Genet.* **9**, 735–744.

Hellsten E., Vesa J., Olkkonen V. M., Jalanko A. and Peltonen L. (1996) Human palmitoyl protein thioesterase: evidence for lysosomal

targeting of the enzyme and distributed cellular routing in infantile neuronal ceroid lipofuscinosis. *EMBO J.* **15**, 5240–5245.

Himeno M., Koutoku H., Tsují H. and Kato K. (1988) Purification and characterization of acid phosphatase in rat liver lysosomal contents. *J. Biochem.* **104**, 773–776.

Howell K. E. and Palade G. E. (1982) Hepatic Golgi fractions resolved into membrane and content subfractions. *J. Cell Biol.* **92**, 822–832.

International Batten Disease Consortium (1995) Isolation of novel gene underlying Batten disease, CLN3. *Cell* **82**, 949–957.

Janes R. W., Munroe P. B., Mitchison H. M., Gardiner R. M., Mole S. E. and Wallace B. A. (1996) A model for Batten disease protein CLN3: Functional implications from homology and mutations. *FEBS Lett.* **399**, 75–77.

Järvelä I., Sainio M., Rantamäki Olkkonen V. M., Carpán O., Peltonen L. and Jalanko A. (1998) Biosynthesis and intracellular targeting of the CLN3 protein defective in Batten disease. *Hum. Mol. Genet.* **7**, 85–90.

Katz M. L., Gao C.-L., Prabhakaram M., Shibuya H., Liu P.-C. and Johnson G. S. (1997) Immunochemical localization of the Batten disease (CLN3) protein in retina. *Invest. Ophthalmol. Vis. Sci.* **38**, 2375–2386.

Kida E., Golabek A. A. and Wiesniewski K. E. (2001) Cellular Pathology and Pathogenic aspects of neuronal ceroid lipofuscinoses. *Adv. Genet.* **45**, 35–68.

Kobayashi R. and Tashima Y. (1989) Visualization of antigen on nitrocellulose membrane by the oxidative coupling reaction of N,N'-dimethyl-p-phenylendiamine and 4-chloro-1-naphthol. *Anal. Biochem.* **183**, 9–12.

Kobayashi T., Stang E., Fang K. S., de Moerloose P., Parton R. G. and Gruenberg J. (1998) A lipid associated with the antiphospholipid syndrome regulates endosome structure and function. *Nature* **392**, 193–197.

Koike M., Shibata M., Ohsawa Y., Kametaka S., Waguri S., Kominami E. and Uchiyama Y. (2002) The expression of tripeptidyl peptidase I in various tissues of rats and mice. *Arch. Histol. Cytol.* **65**, 219–232.

Kominami E., Ezaki J., Muno D., Ishido K., Ueno T. and Wolfe L. S. (1992) Specific storage of subunit c of mitochondrial ATP synthase in lysosomes of neuronal ceroid lipofuscinosis (Batten's disease). *J. Biochem.* **111**, 278–282.

Kremmidiotis G., Lensink I. L., Bilton R. L., Woollatt E., Chataway T. K., Sutherland G. R. and Callen D. F. (1999) The Batten disease gene product (Cln3p) is a Golgi integral membrane protein. *Hum. Mol. Genet.* **8**, 523–531.

Laemmli U.K. (1970) Cleavage of structural proteins during the assembly of the head of bacteriophage T4. *Nature* **227**, 680–685.

Liu F.-T., Zinnercker M., Hamaoka T. and Katz D. H. (1979) New procerures for preparation and isolation of conjugates of proteins and a synthetic copolymer of D-amino acids and immunochemical characterization of such conjugates. *Biochemistry* **18**, 690–697.

Luiro K., Kopra O., Lehtovirta M. and Jalanko A. (2001) CLN3 protein is targeted to neuronal synapses but excluded from synaptic vesicles: new clue to Batten disease. *Hum. Mol. Genet.* **10**, 2123–2131.

Margraf L. M., Boriak R. L., Routheut A. A. J., Cuppen I., Alhilali L., Bennett C. J. and Bennett M. J. (1999) Tissue expression and subcellular localization of CLN3, the Batten disease protein. *Mol. Genet. Met.* **66**, 283–289.

Martin J.-J. (1991) Adult type of neuronal ceroid lipofuscinosis. *Dev. Neurosci.* **13**, 331–338.

Mineki R., Taka H., Fujimura T., Kikkawa M., Shindo N. and Murayama K. (2002) *In situ* alkylation with acrylamide for identification of cysteinyl residues in proteins during one- and two-dimensional sodium dodecyl sulphate-polyacrylamide gel electrophoresis. *Proteomics* **2**, 1672–1681.

Mitchell W. A., Wheeler R. B., Sharp J. D. *et al.* (2001) Turkish variant late infantile neuronal ceroid lipofuscinosis (CLN7) may be allelic to CLN8. *Eur. J. Paediatr. Neurol.* **5**, 21–27.

Mole S. E. (1999) Batten's disease: eight genes and still counting? *Lancet* **354**, 443–445.

Morre D. J. (1971) Isolation of Golgi apparatus. *Methods Enzymol.* **80**, 535–561.

Ohsumi Y., Ishikawa T. and Kato K. (1983) A rapid and simplified method for the preparation of lysosomal membranes from rat liver. *J. Biochem.* **93**, 547–556.

Okazaki I., Himeno M., Ezaki J., Ishikawa T. and Kato K. (1992) Purification and characterization of an 85 kDa sialoglycoprotein in rat liver lysosomal membranes. *J. Biochem.* **111**, 763–769.

Palmer D. N., Martinus R. D., Cooper S. M., Midwinter G. G., Reid J. C. and Jolly R. D. (1989) Ovine ceroid lipofuscinosis: The major lipopigment protein and the lipid binding subunit of mitochondrial ATP synthase have the same NH_2-terminal sequence. *J. Biol. Chem.* **264**, 5736–5740.

Pearce D. A. and Sherman F. (1997) BTN1, a yeast gene corresponding to the human gene responsible for Batten's disease, is not essential for viability, mitochondrial function, or degradation of mitochondrial ATP synthase. *Yeast* **13**, 691–697.

Pearce D. A., Ferea T., Nosel S. A., Das B. and Sherman F. (1999) Action of BTN1, the yeast orthologue of gene mutated in Batten disease. *Nat. Genet.* **22**, 55–58.

Ranta S., Zhang Y., Ross B. *et al.* (1999) The neuronal ceroid lipofuscinoses in human EPMR and mnd mutant mice are associated with mutations in CLN8. *Nat. Genet.* **23**, 233–236.

Rider J. A., Dawson G. and Siakotos A. N. (1992) Perspective of biochemical research in the neuronal ceroid lipofuscinosis. *Am. J. Med. Genet.* **42**, 519–524.

Savukoski M., Klockars T., Holmberg V., Santavuori P., Lander E. S. and Peltonen L. (1998) CLN5, a novel gene encoding a putative transmembrane protein mutated in Finnish variant late infantile neuronal ceroid lipofuscinosis. *Nat. Geneti.* **19**, 286–288.

Sleat D. E., Donnelly R. J., Lackland H., Liu C.-G., Sohar I., Pullarkat R. K. and Lobel P. (1997) Association of mutations in a lysosomal protein with classical late-infantile neuronal ceroid lipofuscinosis. *Science* **277**, 1802–1805.

Takamiya Y., Yanamura W. and Capaldi R. A. (1986) Mitochondrial myopathies involving the respiratory chain: a biochemical analysis. *Ann. NY Acad. Sci.* **488**, 33–43.

Towbin H., Slaehelin T. and Gordon J. (1979) Electrophoretic transfer of proteins from polyacrylamide gels to nitrocellulose sheets: procedure and some applications. *Proc. Natl Acad. Sci. USA* **76**, 4350–4354.

Ueno T., Muno D. and Kominami E. (1991) Membrane markers of endoplasmic reticulum presented in autophagic vacuolar membranes isolated from leupeptin-administrated rat liver. *J. Biol. Chem.* **266**, 18995–18999.

Vesa J., Chin M. H., Oelgeschläger K., Del Isosomppi J. I., Angelica E. C., Jalanko A. and Peltonen L. (2002) Neuronal ceroid lipofuscinoses are connected at molecular level: interction of CLN5 protein with CLN2 and CLN3. *Mol. Biol. Cell* **13**, 2410–2420.

Vesa J., Hellsten E., Verkruyse L. A., Camp L. A., Rapola J., Santavuori P., Hofmann S. L. and Peltonen L. (1995) Mutations in the palmitoyl protein thioesterase gene causing infantile neuronal ceroid lipofuscinosis. *Nature* **376**, 584–587.

Wheeler R. B., Sharp J. D., Mitchell W. A., Bate S. L., Williams R. E., Lake B. D. and Gardiner R. M. (1999) A new locus for variant late infantile neuronal ceroid lipofuscinosis-CLN7. *Mol. Genet. Metab.* **66**, 337–338.